AD-A179 930 CONFIGURATIONS OF CHARGES ON A SPHERE(U) CHEMICAL RESEARCH DEVELOPMENT AND ENGINEERING CENTER ABERDEEN PROVING GROUND MD R H FRICKEL ET AL APR 87 1/1

UNCLASSIFIED CRDEC-TR-87040 F/G 20/3 NL

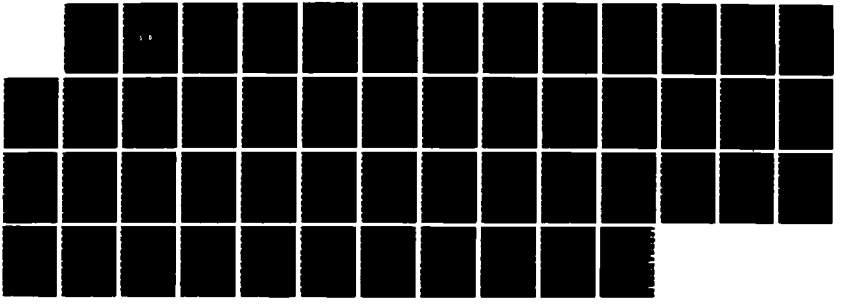

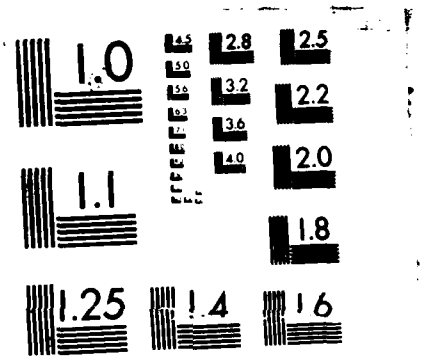

(12)

CHEMICAL RESEARCH, DEVELOPMENT & ENGINEERING CENTER

CRDEC-TR-87040

CONFIGURATIONS OF CHARGES ON A SPHERE

by Robert H. Frickel
Burt V. Bronk
RESEARCH DIRECTORATE

April 1987

U.S. ARMY ARMAMENT MUNITIONS CHEMICAL COMMAND

Aberdeen Proving Ground, Maryland 21010-5423

Disclaimer

The findings in this report are not to be construed as an official Department of the Army position unless so designated by other authorizing documents.

Distribution Statement

Approved for public release; distribution is unlimited.

UNCLASSIFIED

SECURITY CLASSIFICATION OF THIS PAGE

AD-A177 959

REPORT DOCUMENTATION PAGE

1a. REPORT SECURITY CLASSIFICATION UNCLASSIFIED	1b RESTRICTIVE MARKINGS
2a. SECURITY CLASSIFICATION AUTHORITY	3 DISTRIBUTION / AVAILABILITY OF REPORT Approved for public release; distribution is unlimited.
2b. DECLASSIFICATION / DOWNGRADING SCHEDULE	
4. PERFORMING ORGANIZATION REPORT NUMBER(S) CRDEC-TR-87040	5. MONITORING ORGANIZATION REPORT NUMBER(S)
6a. NAME OF PERFORMING ORGANIZATION CRDEC 6b OFFICE SYMBOL (If applicable) SMCCR-RSP-B	7a. NAME OF MONITORING ORGANIZATION
6c. ADDRESS (City, State, and ZIP Code) Aberdeen Proving Ground, MD 21010-5423	7b. ADDRESS (City, State, and ZIP Code)
8a. NAME OF FUNDING / SPONSORING ORGANIZATION CRDEC 8b. OFFICE SYMBOL (If applicable) SMCCR-RSP-B	9. PROCUREMENT INSTRUMENT IDENTIFICATION NUMBER
8c. ADDRESS (City, State, and ZIP Code) Aberdeen Proving Ground, MD 21010-5423	10. SOURCE OF FUNDING NUMBERS PROGRAM ELEMENT NO.: PROJECT NO.: 1L161102 TASK NO.: A71A WORK UNIT ACCESSION NO.: WA03

11 TITLE (Include Security Classification)
Configurations of Charges on a Sphere

12 PERSONAL AUTHOR(S)
Frickel, Robert H., and Bronk, Burt V.

13a. TYPE OF REPORT	13b. TIME COVERED	14. DATE OF REPORT (Year, Month, Day)	15. PAGE COUNT
Technical	FROM 85 Nov TO 86 Sep	1987 April	51

16 SUPPLEMENTARY NOTATION

17. COSATI CODES		
FIELD	GROUP	SUB-GROUP
20	05	

18. SUBJECT TERMS (Continue on reverse if necessary and identify by block number)
Spherical, charge distribution; Charged droplet; Spherical surface, configurations; Coulomb, interaction; Spherical packing

19 ABSTRACT (Continue on reverse if necessary and identify by block number)

We studied the configurations of mechanical equilibrium for objects that are confined to the surface of a sphere and interact with one another via a Coulomb force. New configurations are obtained when the number of objects varies between 17 and 36. These configurations and others from the published literature are analyzed and classified according to their symmetry.

The degree of symmetry has a semiquantitative relationship with the interaction energy. The relationship of this problem to surface problems of aerosols and the configuration of agglomerates is briefly discussed.

20 DISTRIBUTION / AVAILABILITY OF ABSTRACT ☑ UNCLASSIFIED/UNLIMITED ☐ SAME AS RPT. ☐ DTIC USERS	21. ABSTRACT SECURITY CLASSIFICATION UNCLASSIFIED
22a NAME OF RESPONSIBLE INDIVIDUAL TIMOTHY E. HAMPTON	22b TELEPHONE (Include Area Code) (301) 671-2914 22c. OFFICE SYMBOL SMCCR-SPS-T

DD FORM 1473, 84 MAR 83 APR edition may be used until exhausted. All other editions are obsolete.

SECURITY CLASSIFICATION OF THIS PAGE

UNCLASSIFIED

PREFACE

The work described in this report was authorized under Project 1L161102A71A WA03, Aerosol Science. This work was started in November 1985 and completed in September 1986.

The use of trade names or manufacturers' names in this report does not constitute an official endorsement of any commercial products. This report may not be cited for purposes of advertisement.

This report has been approved for release to the public.

CONTENTS

LIST OF FIGURES

LIST OF TABLES

CONFIGURATIONS OF CHARGES ON A SPHERE

1. INTRODUCTION

The relative location of molecules or complexes of molecules on the surface of a spherical aerosol droplet is expected to affect the physical properties of that droplet. Scattering interactions of the particle with laser light or interaction of the particle with the surrounding medium may be affected. Methods for determining ordered configurations on the surface of a sphere are of interest because the curved geometry of the surface may cause substantial differences in the physics of phase changes when the droplets become small with respect to the size of the surface groups considered. It is convenient for several reasons to begin such studies with the consideration of equilibrium arrangements for charges or charged particles that interact with each other via Coulomb forces and are constrained to remain on the surface of a sphere. First, the arrangements determined in this way can be shown to be mathematically related to those determined by the complicated forces that are more commonly observed to act between molecules. Further, we expect the computer methods developed for this particular problem to be applicable to the more general problem. Finally, the Coulomb problem is of interest in itself, because droplets with a few elementary charges are common in naturally occurring aerosols, while droplets with as many as several thousand elementary charges are studied in single particle experiments using electrodynamic balances.

In this report, we consider the configurations of charges that interact via Coulomb forces and are constrained to remain on the surface of a sphere. Because no energy exchange with the droplet or surrounding medium is considered, the polyhedra resulting are the "crystals" of charges at zero degrees Kelvin. This problem is closely related to the more general problem of finding the minimum energy configuration on a sphere for particles interacting with energy

$$E = \frac{1}{2}\sum_{i=1}^{n}\sum_{\substack{j=1 \\ j\neq i}}^{n}\left|\bar{r}_i-\bar{r}_j\right|^{-m} \qquad (1)$$

where n is the number of particles and $\bar{r}_i$ is the position of the i^{th} particle and $\left|\bar{r}_i\right| = 1$, i=1 to n, and the present problem represents the case with m = 1. The general problem was reviewed by Melnyk et al.,[1] who also discuss the relationship among the equilibrium figures for various values of m, and point out that as m becomes very large, the calculation gives the configuration for the closest packing of inflexible circles on a sphere. The equilibrium figures for the various values of m are related, so that the calculations and methods discussed here are related to numerous other problems in small particle chemistry and physics such as the minimum-energy configuration for an arrangement of atoms surrounding a central cluster for which $n \approx 6$ is most appropriate, as pointed out by Clare and Kepert,[2] who also review the inflexible circle case for n up to 40. The problem of closest packing of inflexible circles on a sphere has not been solved in the infinite limit, but one might expect that the solution will resemble the well-known case of closest packing of equal inflexible circles in the plane which is hexagonal (see for example Segre and Mahler[3] for a proof using elementary methods). Berezin[4] shows that the configurations assumed by charged particles on a sphere give realizable examples of important problems in statistical mechanics, as exemplified by the configurations attained in the presence of a uniform external electric field.

Foeppl[5] addressed the Coulomb case (m=1) for n = 2 through 8, 10, 12, and 14; Melnyk[1] presents results for n = 2 through 16. Berezin[6] observes that the cube and the dodecahedron are not equilibrium configurations. We reexamine these cases with the present calculational method and determine additional equilibrium configurations for particle numbers up to n = 32. Details of the symmetry for each equilibrium figure are presented in Section 3. Because the regular tetrahedron, octahedron, and icosahedron are of recurring importance, the symmetries of these figures are reviewed.

2. APPROACH

It is desired to find the configuration of n like equal charges on the surface of a unit sphere such that the energy E is minimized:

$$E = \frac{1}{2}\sum_{i=1}^{n}\sum_{\substack{j=i \\ j\neq 1}}^{n} \frac{1}{\left|\bar{r}_i - \bar{r}_j\right|} \tag{2}$$

The center of the sphere is $\bar{O} = (0,0,0)$, and the i^{th} charge is located at $\bar{r}_i$ where $\left|\bar{r}_i\right| = 1$. The configurations are computed by arbitrarily specifying the positions of the charges on the surface of the sphere and then recursively displacing each charge by a displacement proportional to the tangential force on it due to all the other charges. To this end the tangential force on each charge is calculated:

$$\bar{T}_i = \bar{r}_i \times (\bar{F}_i \times \bar{r}_i) \tag{3}$$

Here

$$\bar{F}_i = \sum_{\substack{j=1 \\ j\neq i}}^{n} \frac{\bar{r}_{ij}}{r_{ij}^3} \tag{4}$$

where $\bar{r}_{ij} = \bar{r}_i - \bar{r}_j$ and $r_{ij} = \left|\bar{r}_{ij}\right|$. A small displacement is then calculated for the charge via

$$\overline{dr}_i = \bar{F}_i dt \tag{5}$$

where dt is a preselected "time" interval. This procedure is reiterated until the largest among the n values of dr_i is less than a predetermined convergence value ds. This system is actually a scheme to minimize E numerically but may be regarded physically as computation of the motion of each charge in the electrostatic field of the others in the presence of drag great enough that the acceleration term can be neglected, in which case dt contains the reciprocal of the drag coefficient as a factor.

The choice of the value of dt depends to a certain extent on the number of charges, the value of dt is around 0.1. If dt is too small, convergence is unnecessarily slow; if dt is too large, the charges tend to wander aimlessly over the surface of the sphere. In some cases the original charge configuration was set at an equilibrium position not at the minimum energy. In this situation, if dt is too small in relation to the convergence value ds, the charges do not leave the original configuration; if dt is somewhat larger, the charges leave the original configuration, slowly at first, then with increasing speed, and finally converge to the minimum-energy configuration. The question of whether the equilibrium configurations not at minimum energy are local minima or saddle points was not addressed except for the cubic configuration of eight charges; this configuration can be shown to be a saddle point.

Except in one instance for the 32-charge configuration, discussed below, this scheme produced unique equilibrium configurations that, when compared with rival minimum-energy candidates, always had the lower energy.

The resulting configurations are displayed using equal-area projections of the two hemispheres containing the configuration. The upper and lower circles in the illustrations represent the upper and lower hemispheres, respectively. Each hemisphere is viewed from above, so that if the patterns in the upper and lower circles of the representation are identical, the equatorial plane of the configuration is a reflection plane. Vertices and edges lying in the equatorial plane are shown in both hemispheres.

The edges of the polyhedron formed by the points locating the charges are collected into sets of edges of equal length. Each of the sets characterized by the 10 shortest lengths is defined by a unique line type; edges longer than this, if present, are all represented the same way. The reader can see the symmetries involved from the distribution of the various edge types. Figure 1 displays the line types in order of increasing edge length.

The potential energies of the individual charges in each configuration are computed as

$$E_i = \sum_{\substack{j=1 \\ j \neq i}}^{n} \frac{1}{r_{ij}} \tag{6}$$

whence the total potential energy of the configuration is

$$E = \frac{1}{2} \sum_{i=1}^{n} E_i \tag{7}$$

The total configuration energy varies slowly with the positions of the charges. When either of the angular coordinates of one of the charge locations is changed by 1 degree, the *configuration energy changes* in about the sixth significant figure; a 0.1-degree change produces a configuration energy change in the eighth significant figure.

The equilibrium configurations and their symmetries are summarized in Table 1. The values of θ, ϕ, and E_i for each charge and the total energy for the configuration are displayed in Tables 2-31. These tables are displayed at the end of this report.

3. DISCUSSION AND RESULTS

The computed charge configurations can be classified and discussed according to the symmetry they display. The highest symmetry found among the three-dimensional configurations was icosahedral; the lowest consisted of either a single C_2 rotation axis or a single reflection plane.

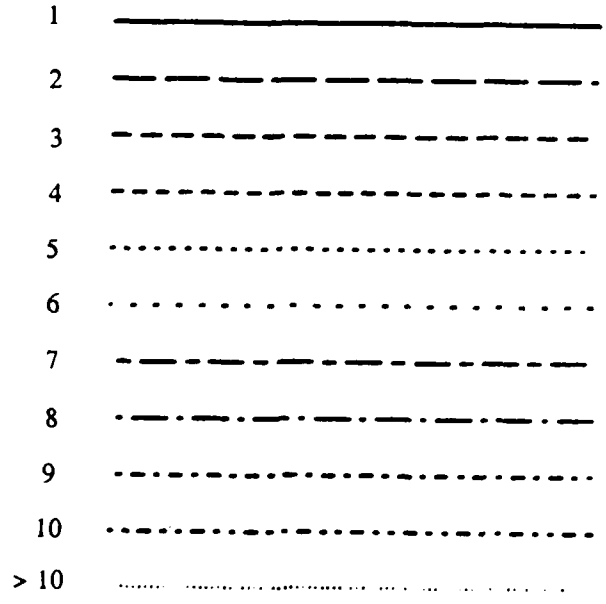

Figure 1. Line Types Denoting Increasing Length

3.1 *Simple D_n Symmetries.*

When only two charges are present, they place themselves at opposite ends of a diameter, whereas three charges distribute themselves on a great circle in an equilateral triangle. The configuration for five charges is a combination of these two: a pair of charges at opposite ends of a diameter and three charges on an equilateral triangle on the great circle lying on the plane perpendicular to the diameter defined by the first two charges. This general type of symmetry recurs frequently in this study, and the diameter so defined is usually regarded as the polar axis (the positions of the points being described by spherical polar coordinates). This 5-charge configuration has D_3 symmetry; that is, the polar axis is C_3, and there are three C_2 axes perpendicular to it, $2\pi/3$ radians apart. The equatorial ($\theta=\pi/2$) plane is a reflection plane, and there are three reflection planes through the polar axis $\pi/3$ radians apart. There is inversion about the center of the sphere. The symmetry of the 6- and 7-charge configurations are similar; the equatorial polygon is a square for the 6-charge figure and a pentagon for the 7-charge figure, with corresponding differences in the symmetry axes and the number of vertical reflection planes. There are two sets of equivalent points in the 5- and 7-charge configurations, namely the polar set and the equatorial set; charges on equivalent points have equal energies. The 6-charge figure is a regular octahedron and is discussed in Section 3.3. The 5-, 6-, and 7-charge configurations are shown in Figure 2.

3.2 *Tetrahedral Symmetry.*

Four charges arrange themselves into a tetrahedron. In the case of tetrahedral symmetry we will regard the $\theta = 0$ pole as the site of one of the four corners; the remaining corners lie on the corners of an equilateral triangle in the horizontal plane at $\theta = \arccos(-1/3)$. Through each of the four corners and perpendicular to its opposite face is a C_3 rotation axis (one of these is the polar axis). There is a reflection plane (through the center of the figure) perpendicular to each of the six edges. Connecting the midpoints of and perpendicular to each of the three pairs of noncoterminous edges is an S_4 axis; that is, if the figure is rotated about the axis by $(2\pi)/4$ radians and then reflected in the plane perpendicular to that axis, the figure remains unchanged. The three S_4 axes are mutually perpendicular. All points on the tetrahedron are equivalent. Tetrahedral symmetry occurs in all five of the regular polyhedra; however, not all regular polyhedra are minimum-energy configurations.

The 22- and 28-charge configurations also display tetrahedral symmetry. The 22-charge configuration consists of a charge at each corner of a tetrahedron surrounded by a nonplanar hexagon, three of whose corners are shared with the hexagons surrounding the other corners. The hexagons are symmetrical with respect to the reflection planes of the tetrahedron, so that the whole configuration has all the symmetries of the tetrahedron. On the other hand, the corner hexagons of the 28-charge configuration, which are not connected with their neighbors, are rotated about their corresponding C_3 axes in such a way that the reflection planes are destroyed. This configuration retains the rotation axes of the tetrahedron but not the S_4 axes nor the reflection planes. There are three sets of equivalent points in the 22- and 28-charge configurations.

Figure 3 shows the three tetrahedral configurations viewed toward a corner; the C_3 symmetry can be seen in all three figures, as well as three of the six reflection planes. In Figure 4, the 22- and 28-charge figures are shown with only two edge-length sets displayed, so that the tetrahedral structure may be seen more clearly; the corners of the tetrahedron are at the junctures of the triplets of solid-lined edges. Figure 5 displays the three configurations viewed toward an edge; the S_4 axis can be seen in the 4- and 22-charge configurations, as well as its failure to appear in the 28-charge figure.

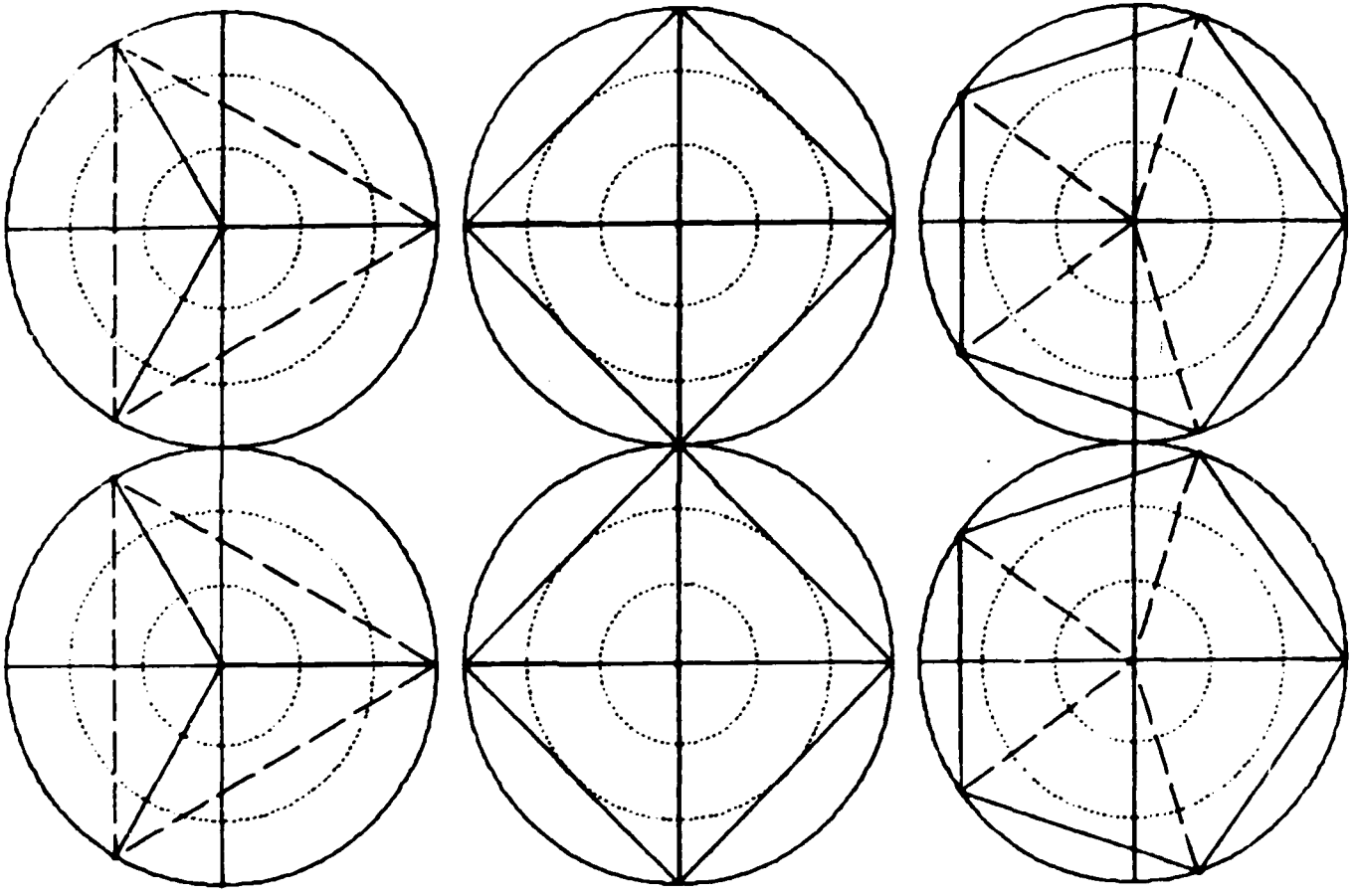

a. 5 charges: D_3 b. 6 charges: D_4 c. 7 charges: D_5

Figure 2. D_n Bipyramids

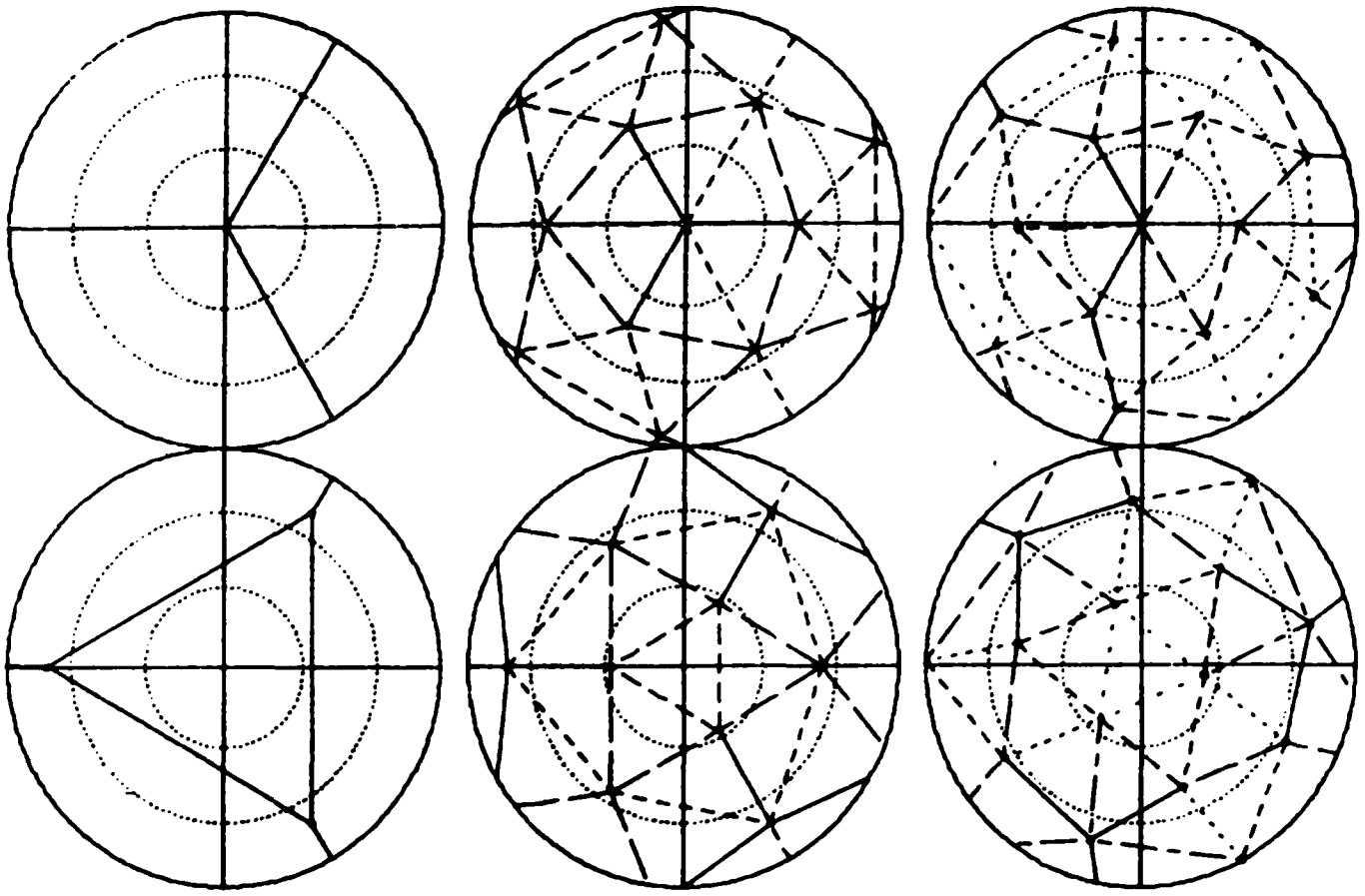

a. 4 charges (tetrahedron)

b. 22 charges (tetrahedral symmetry)

c. 28 charges (tetrahedral rotational symmetry, no reflections)

Figure 3. Tetrahedral Symmetry (viewed toward a corner, showing C_3 Symmetry)

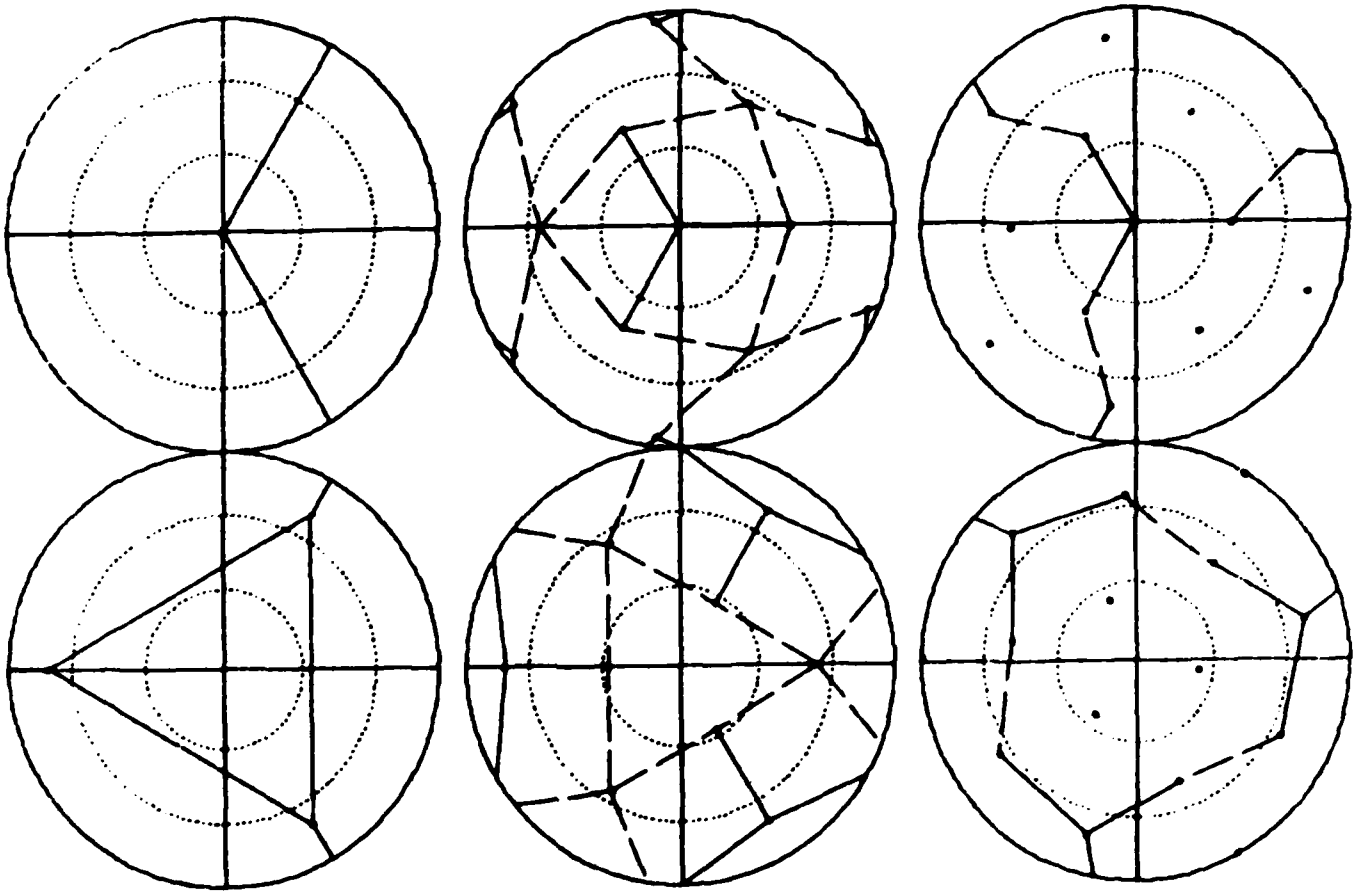

a. 4 charges

b. 22 charges

c. 28 charges

(some edges are not shown to more clearly show the tetrahedral symmetry)

Figure 4. Tetrahedral Symmetry (viewed toward a corner)

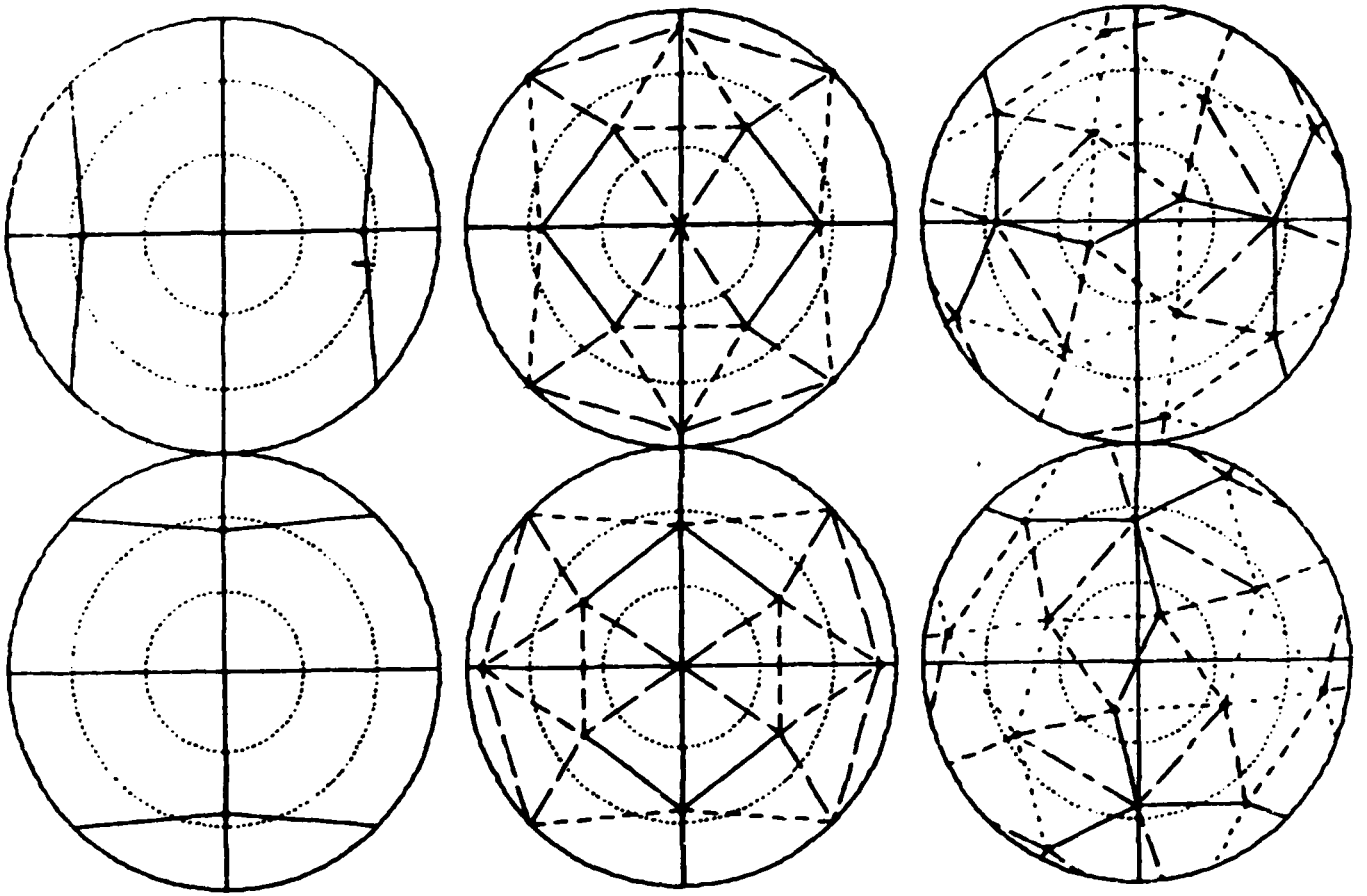

a. 4 charges b. 22 charges c. 28 charges

(C_2 axes can be seen; S_4 axes are apparent in a and b, missing in c)

Figure 5. Tetrahedral Symmetry (viewed toward an edge)

3.3 *Octahedral Symmetry.*

The 6-charge configuration is the regular octahedron, consisting of points at $\theta = 0$ and $\theta = \pi$ and four points situated on a square at $\theta = \pi/2$. Each of the three mutually perpendicular axes joining two diametrically opposed points is a D_4 axis. There is a reflection plane perpendicular to each of these axes, and another perpendicular to each of the six pairs of parallel edges -- a total of nine reflection planes. There is an S_6 axis perpendicular to each of the four pairs of opposite faces and joining their centers. There is a C_2 axis perpendicular to each of the six pairs of parallel edges. The centers of two opposite faces above the $\theta = \pi/2$ plane and the centers of the two faces below that plane (not directly below the first two faces) lie on the corners of a tetrahedron; obviously there are two such tetrahedral structures in the octahedron. All points are equivalent.

Partial octahedral symmetry recurs in the 24-charge configuration. This configuration is a slightly distorted snub cube. The centers of the six square faces of this configuration lie at the corners of an octahedron. This configuration has all the rotation axes of the octahedron but none of the reflection planes, because, for example, neither the edges nor the diameters of the square faces are parallel to the (Euclidean) coordinate axes. All the edges of the snub cube are equal and all the points are equivalent. The distortion of the snub cube necessary to produce the minimum-energy figure causes the lengths of the edges to become unequal; the points remain all equivalent.

Figures 6-8 display the 6- and 24-charge configurations viewed toward an octahedral corner, face, and edge, respectively. One can see that the octahedral rotation axes are retained in the 24-charge configuration, but the reflection planes are not. A cube is shown for comparison in each figure, viewed toward the corresponding symmetry axis, because the cube has the same symmetry as the octahedron; the cube is not a minimum-energy configuration. The positions and energies for the cube are presented in Table 32.

3.4 *Icosahedral Symmetry.*

The 12-charge configuration is a regular icosahedron. The icosahedron has six S_{10} axes, one through each opposing pair of vertices, ten S_6 axes, one through the centers of each pair of opposing faces, and fifteen C_2 axes, one parallel to each pair of parallel edges (and perpendicular to another such pair). These C_2 axes induce D_{10} symmetry with respect to the S_{10} axes D_6 symmetry with respect to the S_6 axes. The configuration has 15 reflection planes, one perpendicular to each pair of parallel edges. The 32-charge configuration is related to the rhombic triakontahedron (the dual of the cuboicosahedron), which is not inscribable in a sphere and hence cannot be a configuration of charges on a sphere. The rhombic triakontahedron can be distorted so as to be inscribable in a sphere by bending each rhombus along its shorter diagonal, replacing each rhombic face with two triangular faces. The resulting figure is the 32-charge configuration; it has two sets of equivalent points, namely the 12 vertices of the regular icosahedron and the 20 vertices of the regular dodecahedron (see Tables 10, 30, and 33), and it has icosahedral (or dodecahedral) symmetry. Figure 9 shows the icosahedron viewed toward a vertex, the center of a face, and the midpoint of an edge. Figure 10 shows the 32-charge configuration viewed along the same symmetry axes.

As mentioned above, one computation for 32 charges produced a different equilibrium configuration, shown in Figure 10 and Table 34. This configuration has a higher energy than the triakontahedral configuration, as is shown by comparison of Tables 34 and 30. The starting configuration leading to this anomalous configuration was not recorded, and the configuration did not reappear in the several replications done for 32 charges.

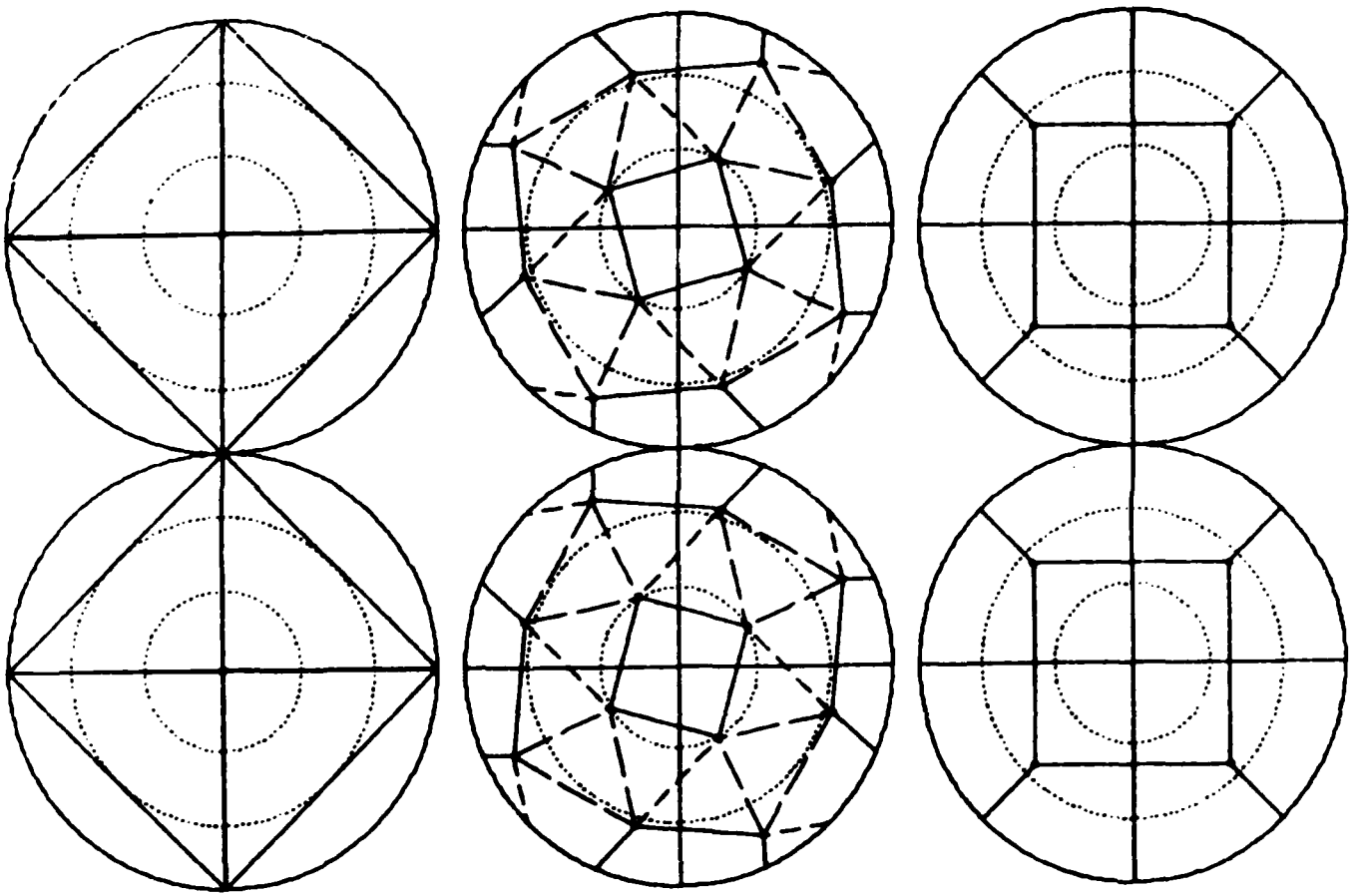

a. 6 charges (octahedron)

b. 24 charges (distorted snub cube)

c. cube (not minimum energy configuration)

(reflection planes present in a and c are missing in b)

Figure 6. Octahedral (cubic) Symmetry (viewed toward octahedral corner; C_4 symmetry)

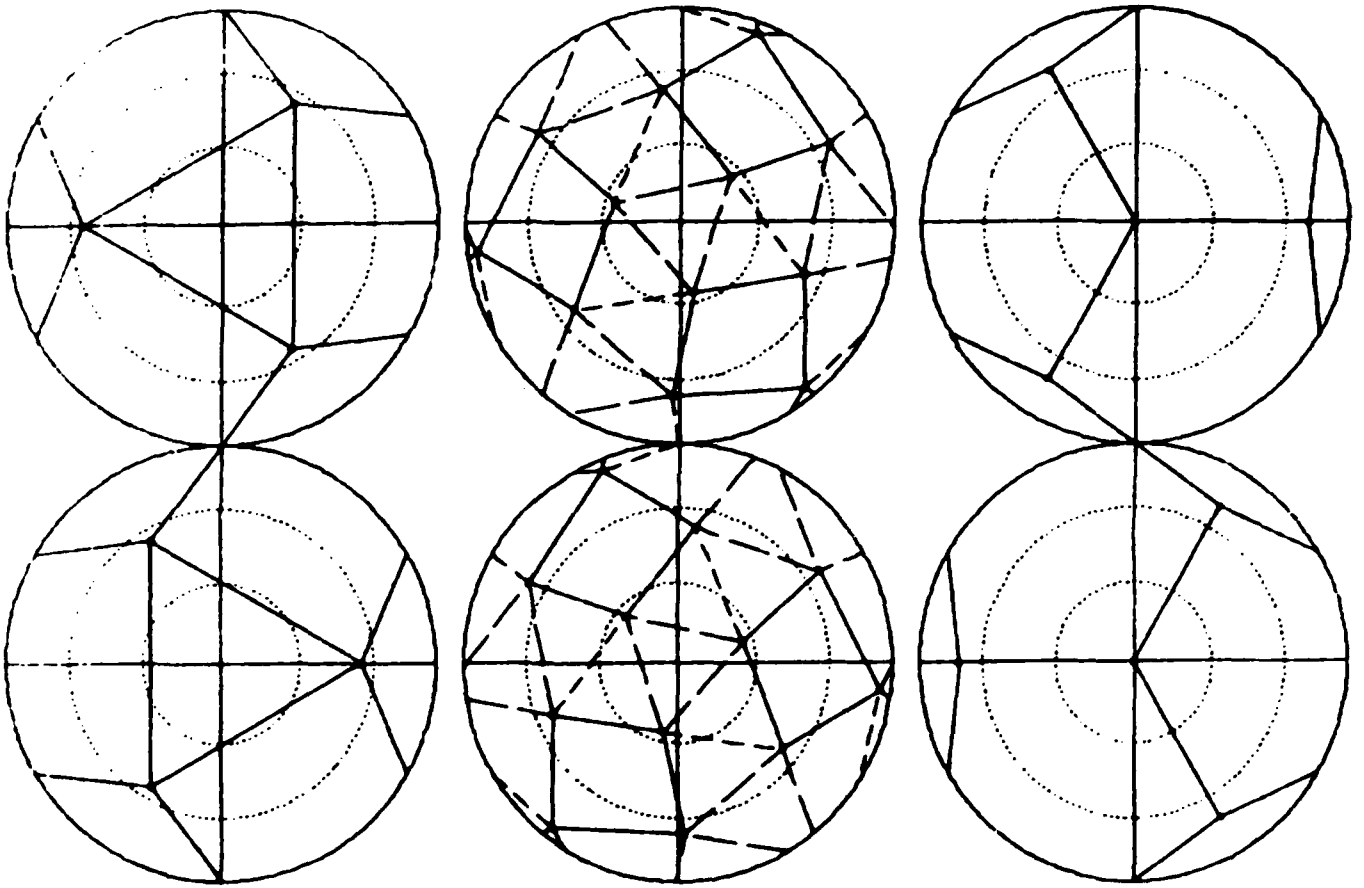

a. 6 charges

b. 24 charges (reflection plane missing)

c. cube

Figure 7. Octahedral Symmetry (viewed toward octahedral face showing C_3 symmetry)

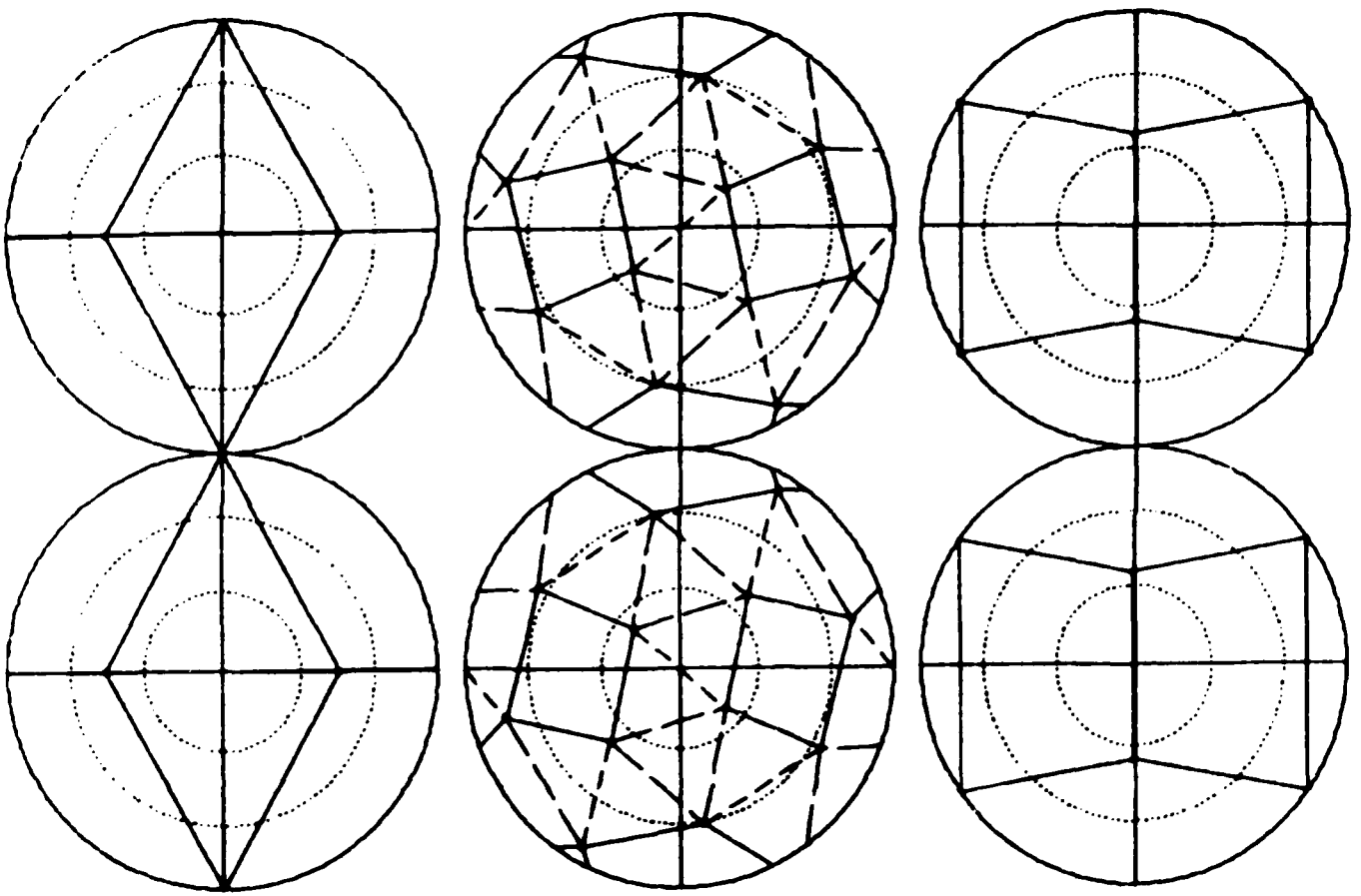

a. 6 charges

b. 24 charges (reflection plane missing)

c. cube

Figure 8. Octahedral Symmetry (viewed toward octahedral edge showing C_2 symmetry)

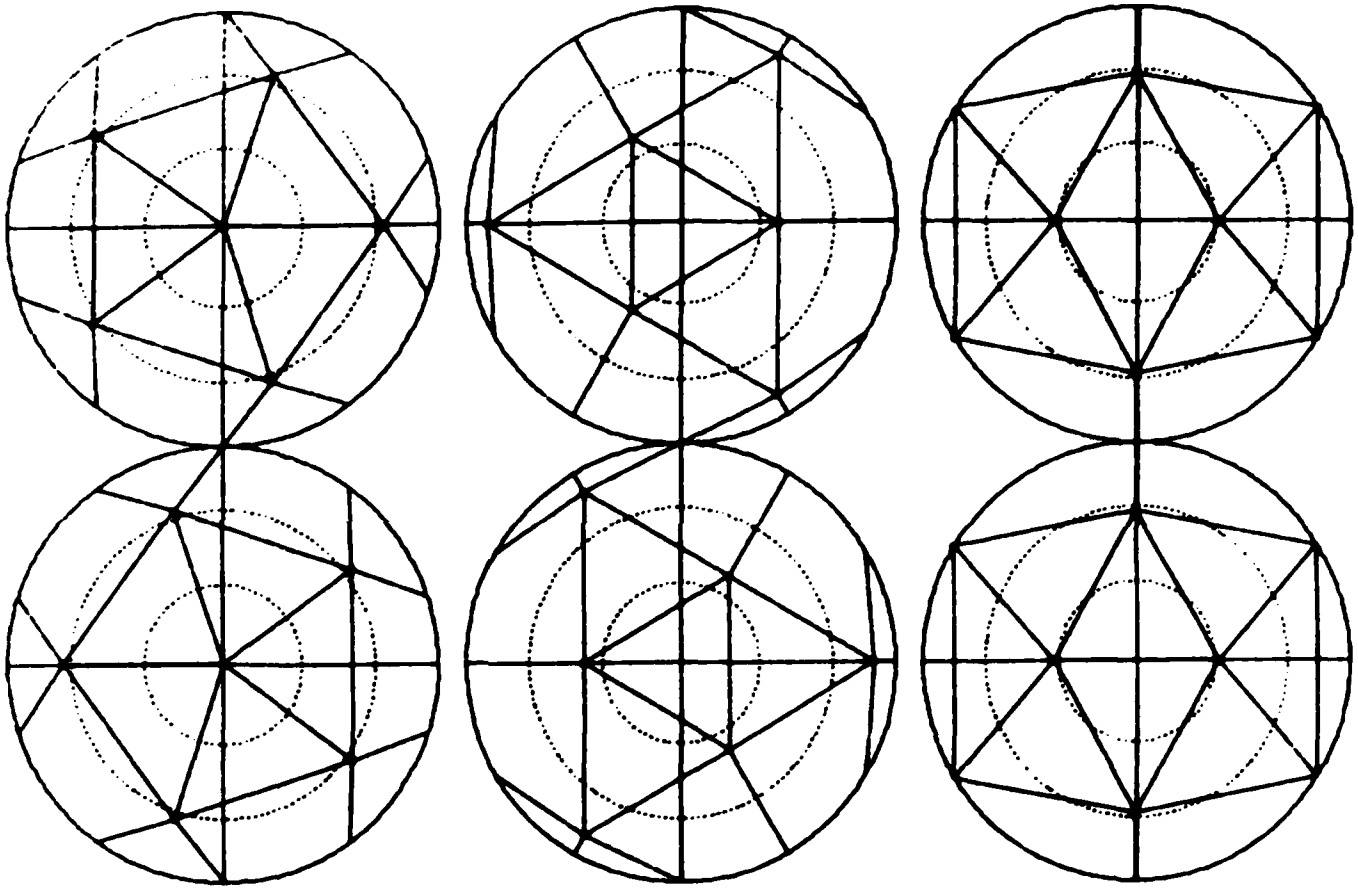

a. S_{10} axis, D_5 Symmetry (viewed toward vertex)

b. S_6 axis, D_3 Symmetry (viewed toward face)

c. C_2 (viewed toward edge)

Figure 9. 12 Charges: Icosahedron

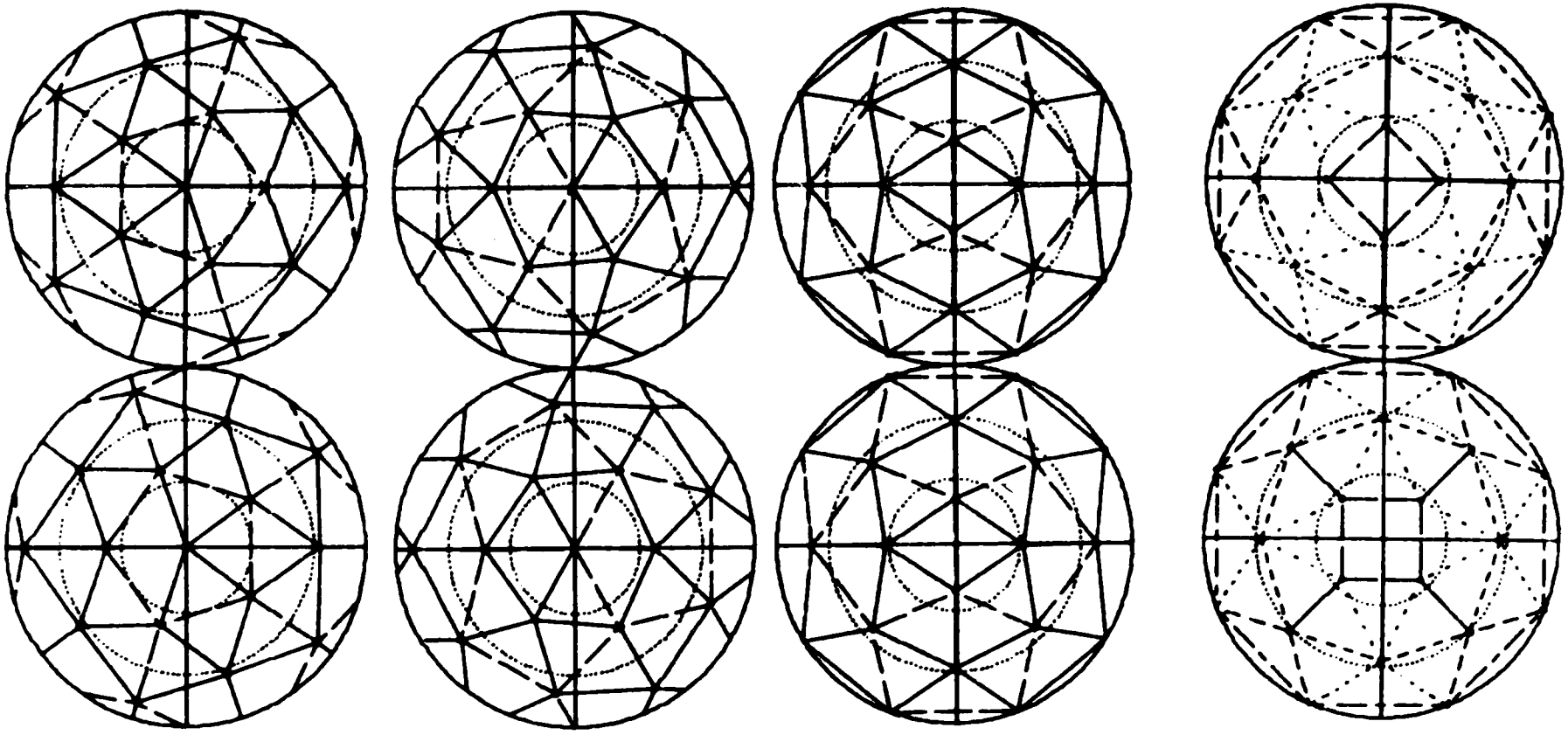

a. S_{10} axis, D_5 Symmetry
(viewed toward icosahedral vertex)

b. S_6 axis, D_3 Symmetry
(viewed toward icosahedral face)

c. C_2 Symmetry
(viewed toward icosahedral edge)

d. Anomalous configuration

Figure 10. Icosahedrally Symmetric and Anomalous 32-Charge Configurations

3.5 *C_3 Symmetry.*

Aside from those displaying tetragonal, octahedral, and icosahedral symmetry, a number of other configurations were found whose most important symmetry element is a C_3 symmetry axis, usually taken to be the polar axis. The 5-charge configuration has already been described as D_3 with one equatorial and three vertical reflection planes. The 9- and 20-charge configurations have the same symmetries. In the 9-charge configuration the polar points are replaced by horizontal triangles. In the 20-charge figure the equatorial points of the 5-charge figure are replaced by a double row of triangles. These three configurations are shown in Figure 11.

The regular dodecahedron also has 20 vertices but is not a minimum-energy configuration. For the most part, a high degree of symmetry tends to be associated with low configuration energy (see Section 3.11), but this is not a general rule, as is exemplified here. The 20-charge minimum-energy polyhedron has, for example, four sets of equivalent points and edges of seven different lengths, as compared with one each for the regular dodecahedron, but nevertheless has a lower configuration energy.

The 15-charge configuration consists of five horizontal triangles and has D_3 symmetry, but the lower hemisphere is rotated slightly about the C_3 axis with respect to the upper, so that all the reflection planes are lost. The 23- and 29-charge configurations have the same symmetry as the 15-charge configuration. These three configurations are shown in Figure 12.

The 31-charge configuration, shown in Figure 13, has C_3 symmetry about the polar axis and three vertical reflection planes. This configuration lacks the horizontal axes necessary for D_3 symmetry.

3.6 *Square Antiprisms (D_4 Symmetry).*

The 8-, 10-, 16-, and 18-charge configurations are S_8 figures related to the square antiprism. The 8-charge figure is a square antiprism; it may be considered as the result of twisting one face of a cube by $\pi/4$ radians about the perpendicular axis through its center; this reduces the energy of the configuration and allows the two remaining parallel square faces to expand and move toward each other, closer to the $\theta = \pi/2$ plane. These relationships are clarified in Tables 8 and 31. The 10-charge configuration consists of a square antiprism with an additional charge at each pole. In the 16-charge figure, the polar charges are replaced by squares centered at the poles. In the 18-charge configuration polar charges are again added. At each incrementation, the previous configuration contracts toward the equatorial plane. These configurations are displayed in Figure 14.

3.7 *C_5 Symmetry.*

The 7-, 17-, and 27-charge configurations consist of constructs of horizontal pentagons, one lying on the equator, and a charge at each pole; all have D_5 symmetry with one horizontal and five vertical reflection planes. They are displayed in Figure 15.

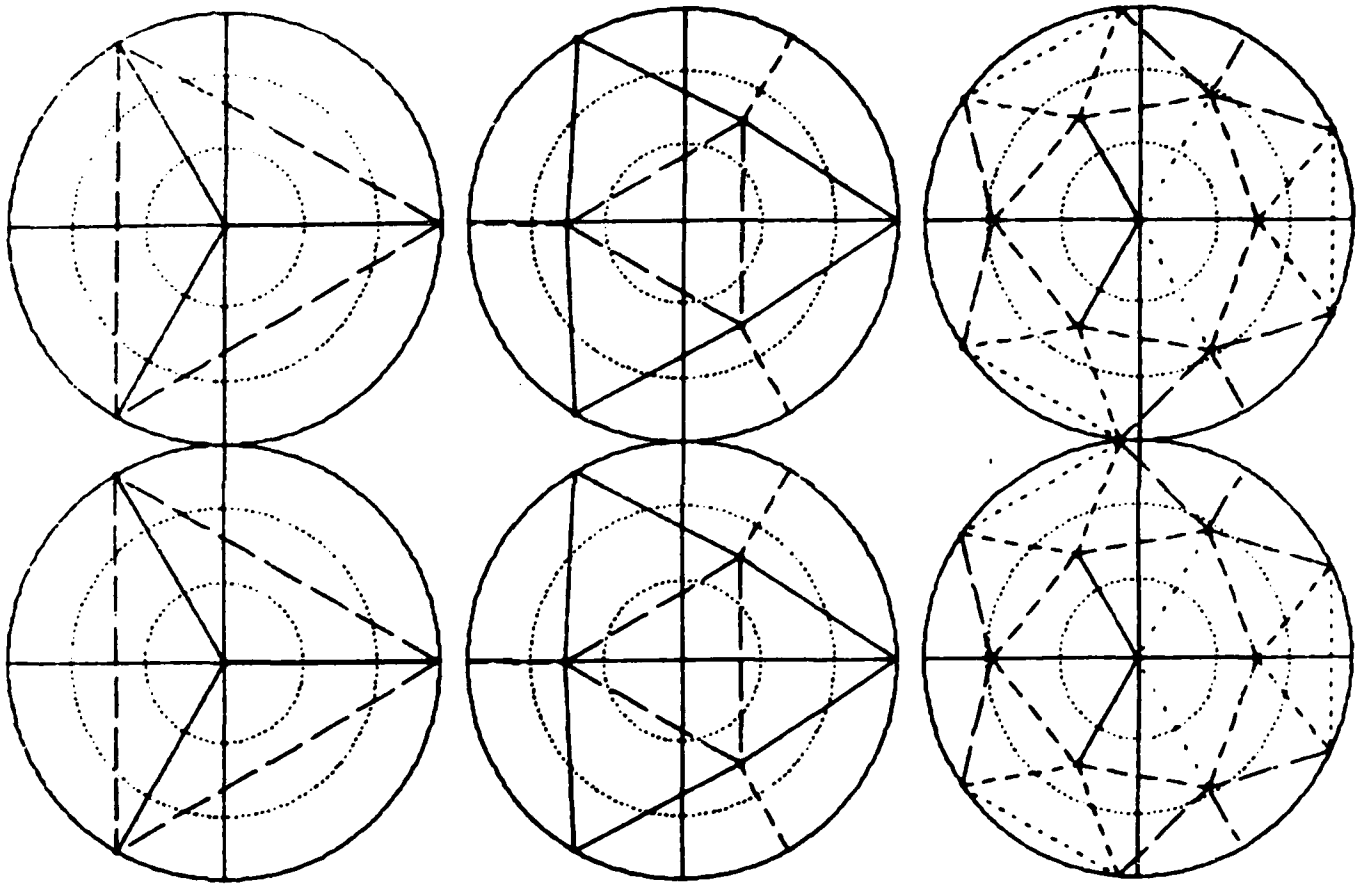

a. 5 charges b. 9 charges c. 20 charges

Figure 11. D_3 Symmetry with Three Vertical Reflection Planes

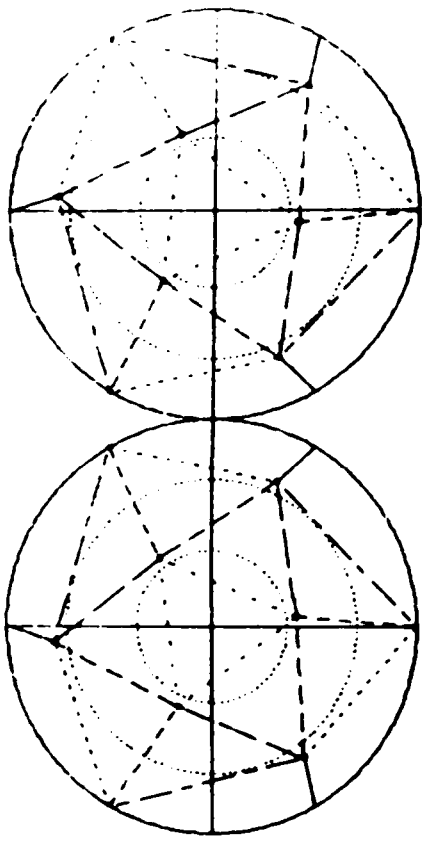

a. 15 charges

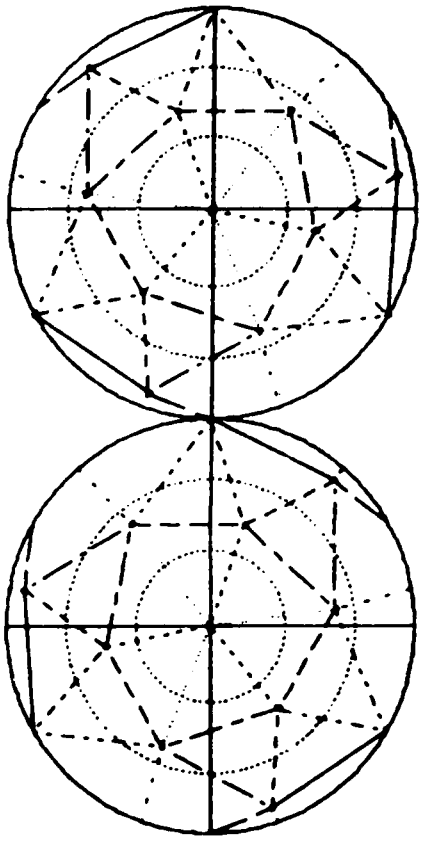

b. 23 charges

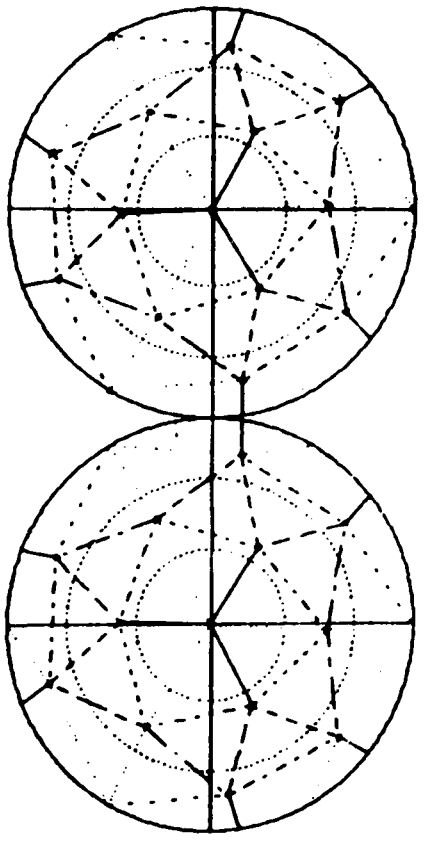

c. 29 charges

Figure 12. D_3 Symmetry Without Reflection Planes

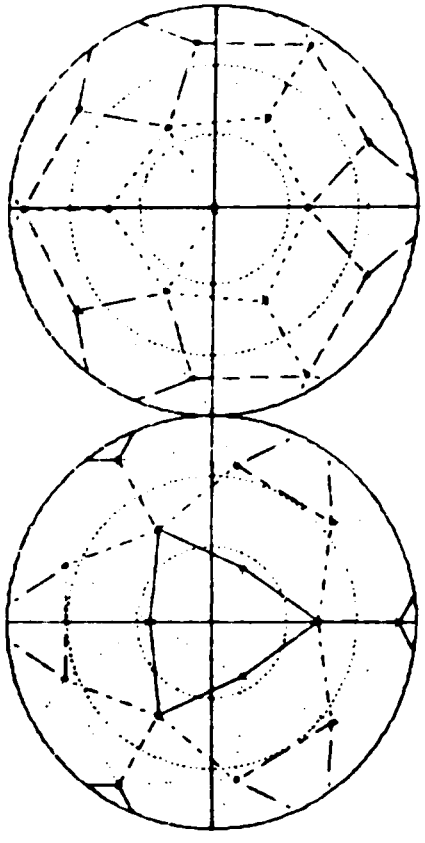

31 charges

Figure 13. C_3 Symmetry with Vertical Reflection Plane

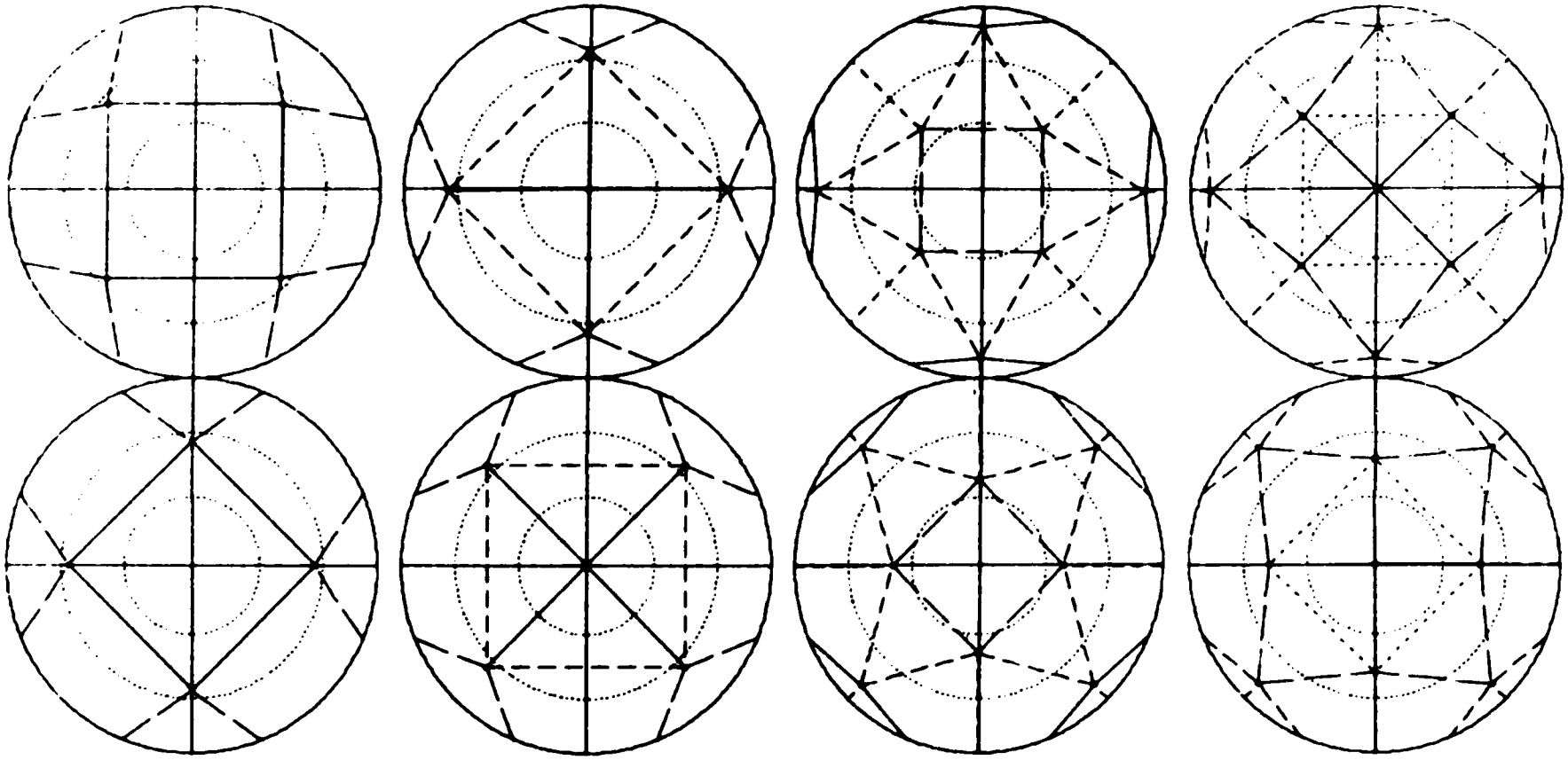

a. 8 charges b. 10 charges c. 16 charges d. 18 charges

Figure 14. D_4 Symmetry (S_8): Square Antiprism

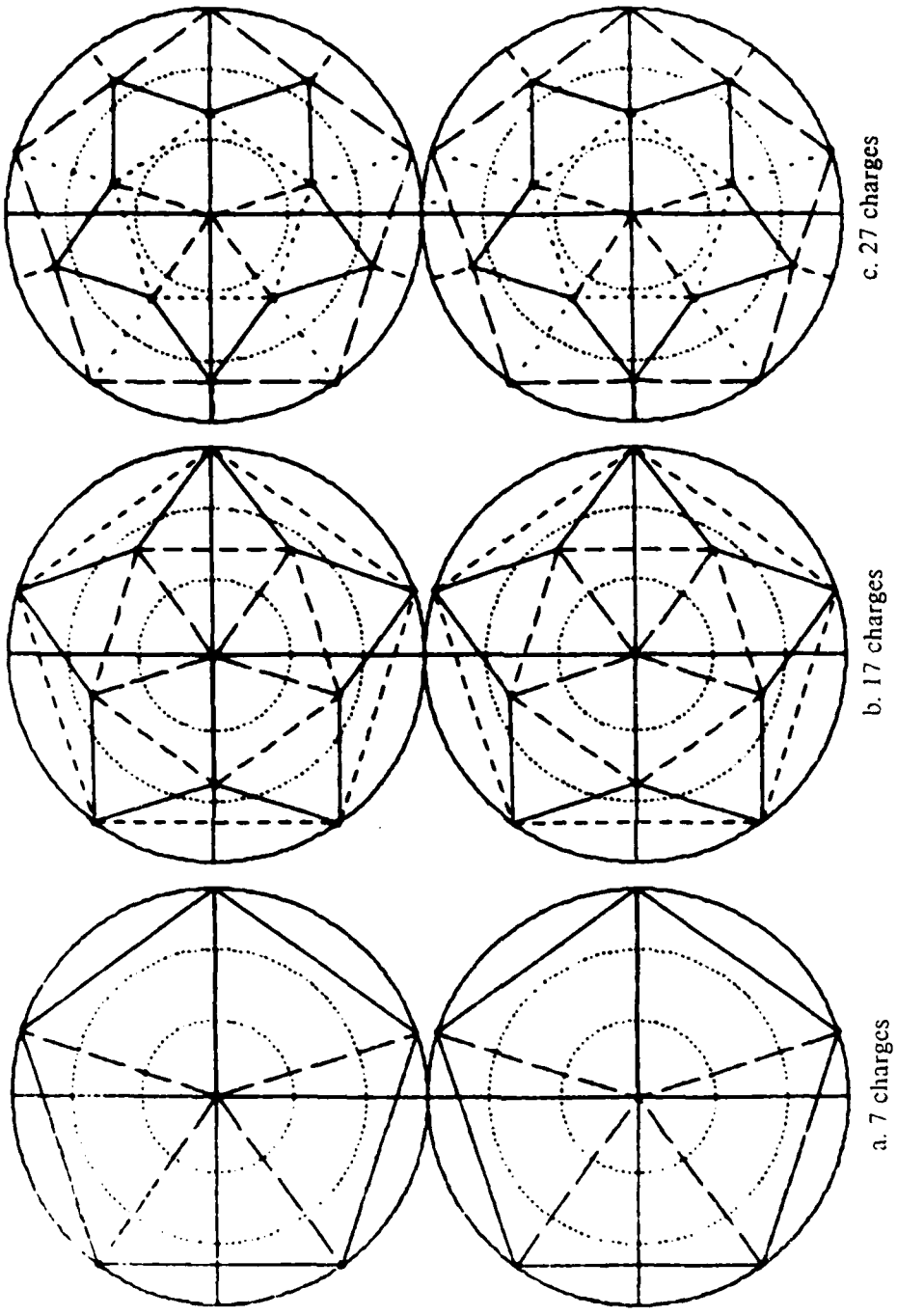

Figure 15. D_5 Symmetry

3.8 *Hexagonal Symmetry.*

The 14-charge configuration was found by Foeppl to consist of a hexagonal antiprism and two polar charges. Melnyk et al. report a configuration with lower energy consisting of a regular octahedron and a square prism; they do not report the angular positions of the horizontal squares of the prism, nor any energies. We searched for Melnyk's minimum-energy configuration by direct calculation of the total energy for configurations consisting of a regular hexagon and two horizontal squares, not necessarily positioned symmetrically above and below the $\theta=\pi/2$ plane and not necessarily oriented the same way within their horizontal planes. We found that, as one would expect, when the horizontal squares are located at any pair of polar angles, say θ_1 and θ_2, their corners must be displaced azimuthally from the corners of the equatorial square of the octahedron by $\pi/4$ radians. Orienting the squares in this way, we then varied θ_1 and θ_2 independently over the range 0 to π, directly calculating the energy of the configuration in each case, and found that the minimal energy occurred when θ_1 and θ_2 were respectively 54.7356 and 126.2644 degrees; these are the polar angles of the corners of a cube oriented so that its edges are vertical and horizontal. A search over a four-dimensional grid of the values of θ_1 and θ_2 and the two values of ϕ for a corner of each square disclosed that the minimum found by varying only θ_1 and θ_2 is a local minimum and not a saddle point for the four variables. This energy, the smallest possible for the configuration described by Melnyk, proved to be higher than that calculated for the minimum-energy hexagonal antiprism configuration. Hence we conclude that Foeppl's configuration was correct. This hexagonal configuration, shown in Figure 16, has a polar S_{12} axis, six horizontal C_2 axes, and six vertical reflection planes; it has D_6 symmetry.

3.9 *C_2 Symmetry with Vertical Reflection Planes.*

The 21-, 11-, 13-, and 19-charge configurations are shown in Figure 17. The 21-charge configuration appears to have C_4 symmetry; in fact, the angular position of the charges varies from C_4 symmetry by fractions of a degree (see Table 19). An effort was made to force the configuration into C_4 symmetry, in a manner similar to that described above with respect to non-minimum equilibrium positions, but the charges always returned to the configuration listed in Table 19. The symmetry is C_2 with two perpendicular vertical reflection planes. The 11-, 13-, and 19-charge configurations have, more obviously, this same symmetry.

3.10 *Lesser Symmetries.*

The 30- and 36-charge configurations have D_2 symmetry. They are shown in Figure 18.

The least symmetrical of the 32 configurations studied are the 25- and 26-charge configurations. The 25-charge configuration, shown in Figure 19, has only a reflection plane, vertical in this particular representation. The quadrilateral near $\theta = 0$ is not a square. It can be seen to be a plane from symmetry considerations; in addition, an appropriate triple product was computed and found to be zero. Note the five charges scattered irregularly on the reflection-plane great circle. The 26-charge configuration, shown in Figure 20, has only a C_2 axis.

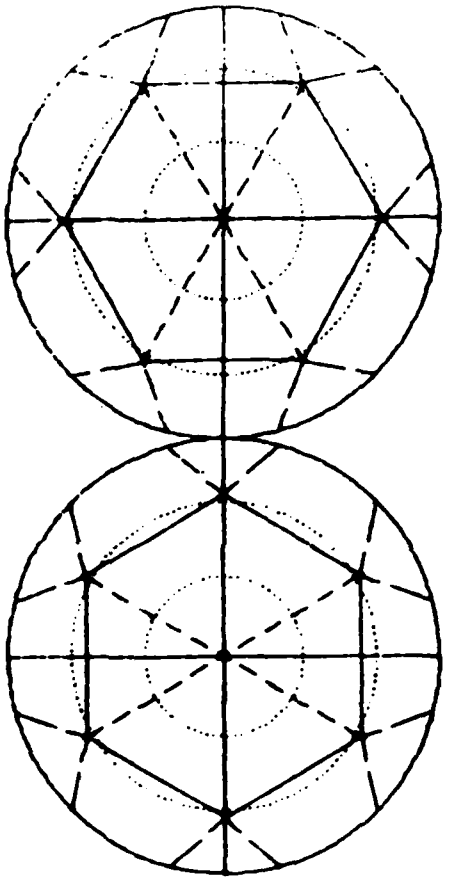

14 charges

Figure 16. D_6 Symmetry (S_{12})

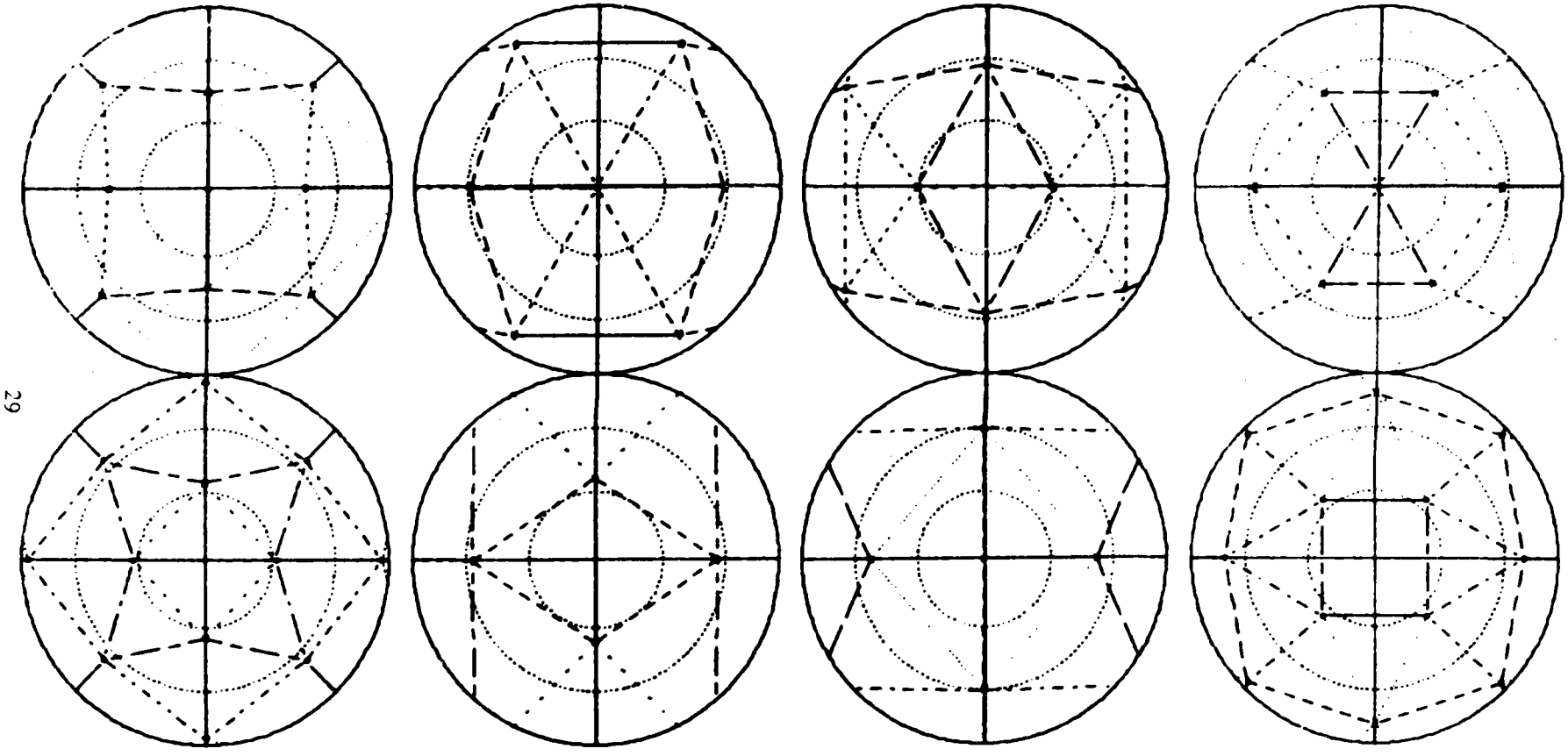

a. 21 charges b. 11 charges c. 13 charges d. 19 charges

Figure 17. C_2 Axis with Vertical Reflection Planes

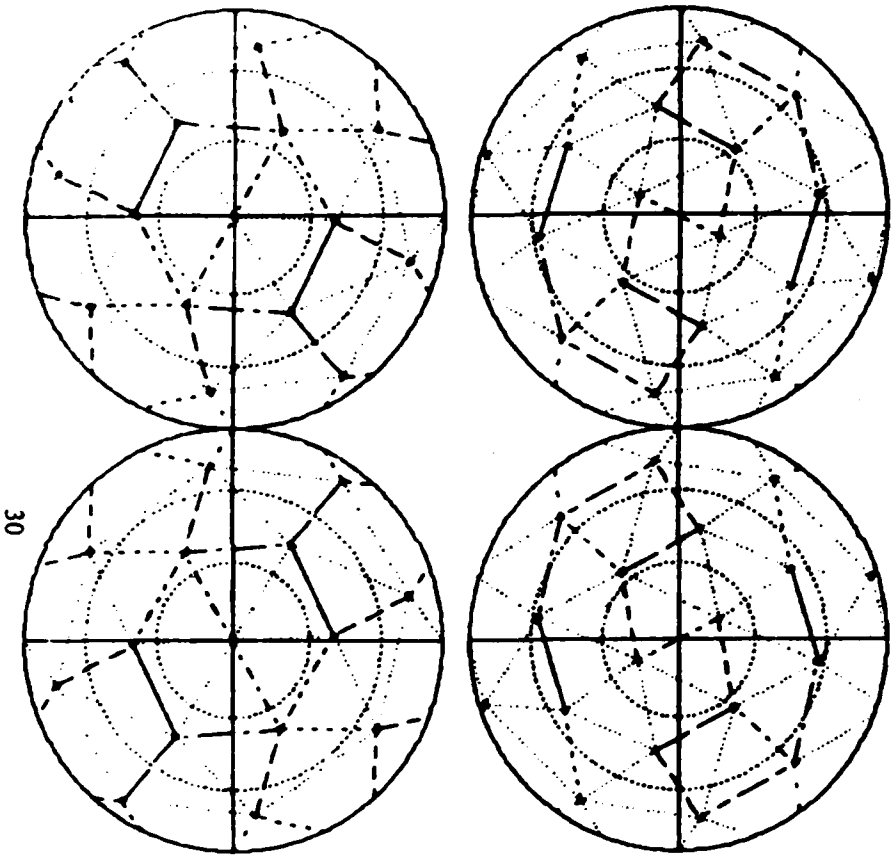

a. 30 charges b. 36 charges

Figure 18. D_2, No Reflection Planes

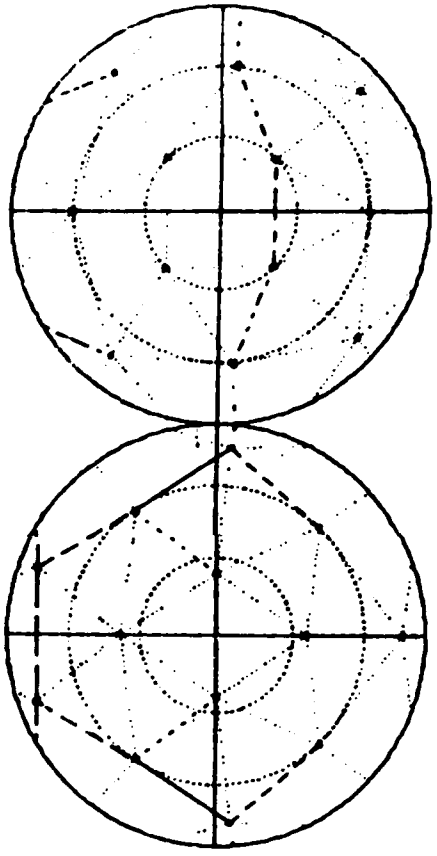

25 charges

Figure 19. One Reflection Plane, No Rotation Axes

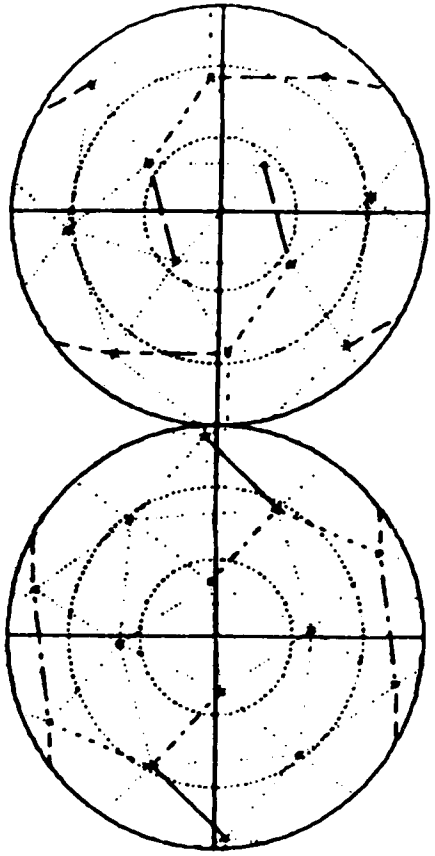

26 charges

Figure 20. C_2 Axis; No Other Symmetry Elements

3.11 *Energy vs Symmetry.*

The energy of a charge of magnitude n uniformly distributed over the surface of a unit sphere is $n^2/2$. The excess of this quantity over the energy E_n of the minimum-energy configuration for n unit charges

$$E_o = n^2/2 - E_n \tag{8}$$

is shown in Figure 21 plotted against n. Figure 22 shows the excess of E_o over a straight line between the points at n=4 and n=36 on the log-log scale. Higher values of this excess correspond to lower values of E_n. Configurations of higher symmetry tend to have higher values than their neighbors, but this comparison cannot be made globally over the whole range of n.

4. CONCLUSIONS AND RECOMMENDATIONS

We have determined a number of new configurations of mechanical equilibrium for a small number of charged particles confined to the surface of a sphere and interacting with a Coulomb force. Each of these appears to be a local minimum and a minimum-energy configuration for the number of charges involved. We have classified these configurations according to symmetry and found that particular symmetries recur over the range of number of charges. We find that although low configuration energy tends to be associated with high symmetry, this is not a general rule and does not appear to be quantifiable.

Other equilibrium configurations exist in many, if not all, of the cases considered. The question as to whether these are real local minima or merely saddle points was not addressed. Neither was the question of proving that a given local minimum is an absolute minimum. The first of these questions can be resolved in a straightforward manner, at least numerically. We expect to accomplish this, at least for several interesting cases. The second question is relatively intractable and does not in general have a known solution.

The problem we have studied leads to zero temperature equilibrium configurations. As pointed out in the introduction, this problem is mathematically related to a number of other problems of physical relevance. A problem of interest to us is the behavior of objects interacting with realistic forces at finite temperatures on the surface of a spherical particle. An attractive initial step to the study of this problem would be to set up computer programs for calculating the molecular dynamics of the system. This computational system can be checked thermodynamically in the ideal gas case and can later be related to situations with more complex interactions and also to the symmetrical configurations studied here as the temperature is reduced sufficiently to induce phase changes.

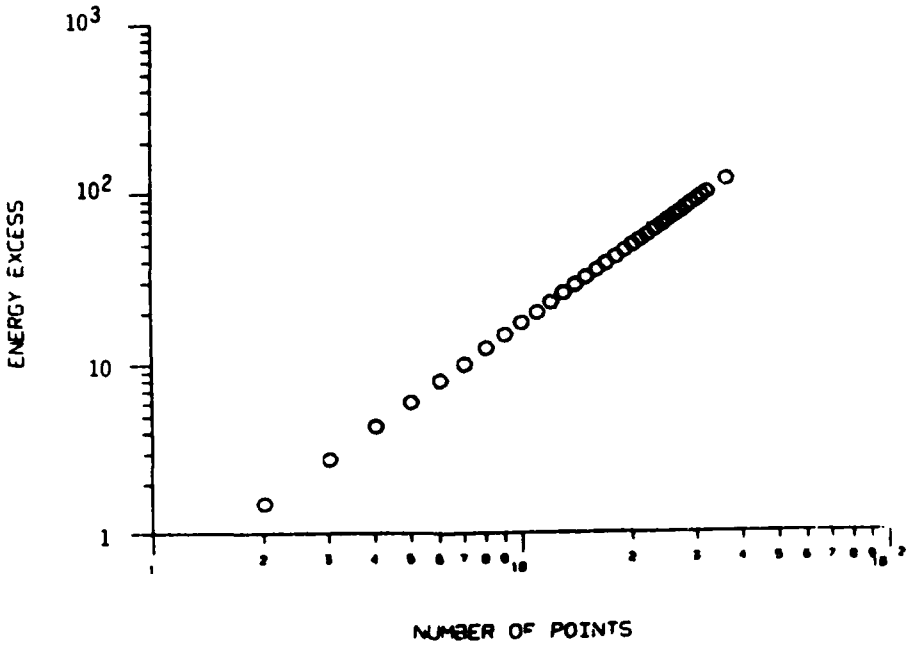

Figure 21. $E_0 = n^2/2 - E_n$ vs n

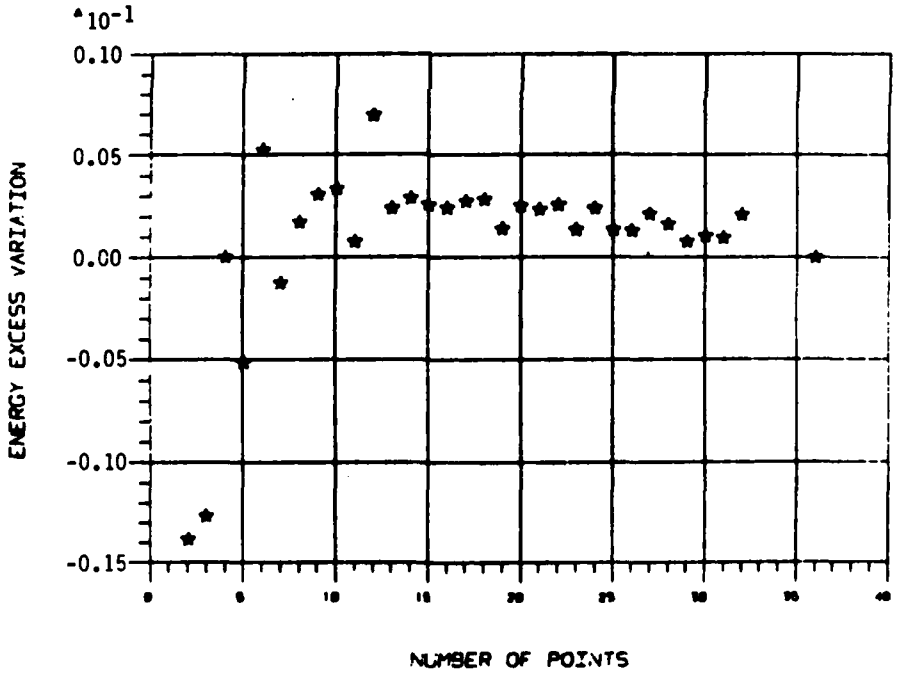

Figure 22. Deviation of E_0 from Straight Line on log-log Plot vs n

Table 1. Equilibrium Configurations

NUMBER OF CHARGES	CHARGE ARRANGEMENTS	SYMMETRIES	NUMBER OF SINGLE CHARGE ENERGIES	TOTAL ENGERY OF INTERACTION	DESCRIPTION OF POLYHEDRON
2	Charges at opposite poles	D_{∞}; Infinite number of vertical reflection planes; horizontal reflection plane	1	0.500000	———
3	Equilateral triangle	D_3; Three vertical reflection planes; horizontal reflection plane	2	1.732051	Plane equilateral triangle
4	Corners of tetrahedron	Full tetrahedral symmetry with reflections	1	3.674235	Regular tetrahedral: 4 triangular faces; 6 equal edges
5	Two at poles, equilateral triangle at equator	D_3 (dihedral) three vertical reflection planes; horizontal reflection plane; inversion	2	6.474691	Double triangular pyramid: 6 faces; 9 edges of 2 different lengths
6	Corners of octahedron	Full octahedral symmetry with reflections	1	9.9852814	Regular octahedron: 8 faces; 12 edges of equal length

7	Two at poles; five at corners of equatorial pentagon	D_5; Five vertical reflection planes; horizontal reflection plane; inversion	2	14.452977	Double pentagonal pyramid 10 triangular faces; 15 edges with 2 different lengths
8	Corners of two parallel squares (one twisted by $\pi/4$ radians) and displaced toward equator from cube configuration (antiprism)	D_4;S_8; Four vertical reflection planes	1	19.675288	Square antiprism ("twisted cube"): 2 square and 8 triangular faces; 16 edges with 2 different lengths
9	Two congruent equilateral triangles above and below equator; one in opposite direction in equatorial plane	D_3 with three vertical reflection planes; a horizontal reflection plane	2	25.759986	14 triangular faces; 21 edges with 3 edge lengths; polar triangles are equilateral; all others are isosceles.
10	Two charges at poles plus corners of square antiprism (closer to equator than for 8 charges)	D_4; S_8 four vertical reflection planes	2	32.716949	Square antiprism with two pyramidal caps; 16 triangular faces; 24 edges with 3 different edge lengths
11	Particles on five different levels as follows (in order from θ=0) 1 at the pole (θ=0) 1 with 2 charges 1 with 4 charges 2 with 2 charges each	C_2; two perpendicular reflection planes	5	40.596450	27 edged polyhedron; 18 triangular faces; 9 different edge lengths

12	Corners of regular icosahedron	Full icosahedral symmetry with reflections	1	49.165253	Regular icosahedron (This is same as pentagonal antiprism with pyramidal polecaps.)
13	Six levels of charges one at the pole 2 with two particles each 1 with four particles 2 with two particles each	C_2; two vertical perpendicular reflection planes	6	58.853231	22 triangular faces; 33 edges with 11 different lengths
14	Two charges at poles; twelve at corners of hexagonal antiprism	D_6; S_{12}; six vertical reflection planes	2	69.306363	Hexagonal antiprism (12 triangular faces) capped by pyramids at poles
15	Charges are at triangular corners of five layers of parallel equilateral triangles; no horizontal reflection plane	D_3	3	80.670244	26 triangular faces; 39 edges with 7 different edge lengths
16	Four layers of squares in two equal sets on corners of two square antiprisms	D_4; S_8; four vertical reflection planes	2	92.920353	Square antiprism capped by squares near poles forming a second square antiprism; 24 triangular and 2 square faces; 40 edges with 4 edge lengths.
17	Two charges at poles; others at corners of three layers of pentagons, one at equator and two congruent above and below equator	D_5; five vertical reflection planes; horizontal reflection plane	3	106.050405	30 triangular faces; 45 edges with 4 edge lengths
18	Same as for sixteen charges plus two at poles	D_4; S_8; four vertical reflection planes	3	120.084467	Same as for 16 charges but with 2 pyramidal caps

19	Seven layers as follows: 1 pole point 4 in rectangle at 50.3° below pole 2 at 57.3° 4 at 94.05° (rectangle) 2 at 101.34° 2 at 109° 4 at 145° (rectangle)	C_2; two vertical reflection planes	7	135.089468	The convex polyhedron has 1 rectangular face and 32 triangular faces
20	Seven layers: two charges at poles; one non-regular hexagon at equator; four equilateral triangles arranged symmetrically about equatorial plane	D_3; three vertical reflection planes; horizontal reflection plane	4	150.881568	The polyhedron has 36 triangular faces giving 54 edges with 7 edge lengths
21	One pole charge; eight layers: 2 4-charge layers 6 2-charge layers	C_2; two vertical (perpendicular) reflection planes	9	167.641622	Charge locations vary from C_4 symmetry by fractions of degrees (eg. several pairs of two layers combine as slightly distorted squares) The polyhedron as 46 triangular faces; 69 edges with 18 different edge lengths
22	Four charges on corners of tetrahedron; six charges on edges; twelve on corners of four equilateral triangles around corners	Full tetrahedral symmetry with reflections	3	185.287536	40 faces; 60 edges with 4 different lengths
23	Two pole points; seven layers of equilateral triangles, one at equator and the others in pairs up and down	D3 (note, no vertical reflection planes)	5	203.930191	42 triangular faces; 63 edges 11 edge lengths

24	Particles arranged so each is at identical corner of square and four triangular faces of the convex polyhedron; one of these triangular faces is equilateral	Octahedral without the 9 possible reflection planes	1	223.347074	Slightly distorted snubbed cube; 8 equilateral and 24 scalene triangles as faces.
25	Five particles nonsymmetically arranged in reflection plane; ten other pairs	One reflection plane only	15	243.812760	45 faces (one quadrilateral); 68 edges with 37 different lengths
26	Charges come in thirteen pairs	C_2 only	13	265.133326	48 triangular faces; 72 edges with 37 different edge lengths
27	Two pole points and five parallel regular pentagons between	D_5; five vertical reflection planes and a horizontal reflection plane	4	287.302615	50 triangular faces; 75 edges having 6 different edge lengths
28	One charge on each of four tetrahedral corners; each surrounded by two different equilateral triangles (seven charges per corner of the tetrahedron)	Tetrahedral rotational symmetry; no S_4 axes, nor reflection planes	3	310.491542	52 triangular faces , four equilateral; 78 edges with 7 different lengths. Reflection symmetry is destroyed by lack of symmetry of the nonplanar hexagons.
29	Two charges at poles; corners of eight equilateral triangular layers in four pairs above and below equator. A ninth equilateral triangle is at equator.	D_3; no horizontal reflection plane no vertical reflection planes.	6	334.634439	54 triangular faces to convex polyhedron giving 81 edges with 14 different edge lengths

30	Two charges at poles; fourteen two layers coming in equivalent pairs above and below equator (i.e. sets of four points with equal energies)	D_2	8	359.603946	58 triangular faces; 87 edges with 17 different lengths
31	One charge at pole; two layers of six equivalent charges; six layers of three equivalent charges in equilateral triangles	C_3 with three vertical reflection planes; No symmetry between upper and lower hemispheres	9	385.530838	66 triangular faces; 99 edges with 26 different lengths
32	Twenty charges at ends of the ten three-fold axes; twelve charges at ends of the six, five fold (S_{10}) axes. The twelve charges are at the corners of a regular isocahedron; the twenty at the corners of a regular dodecahedron	Full icosahedral (with reflections adjoined)	2	412.261275	60 triangular faces; 90 edges with 2 different lengths. This figure is the rhombic *triakontahedron* distorted slightly so as to be inscribable on a sphere.
36	Nine sets of four equivalent charges, each set with two above and two below equator	D_2	9	529.122408	66 triangular faces; 99 edges with 26 different lengths

Table 2. 4 Points

i	θ_i	ϕ_i	E_i
1	.0000	116.5651	1.837117
2	109.4712	.0000	1.837117
3	109.4712	120.0000	1.837117
4	109.4712	-120.0000	1.837117

Configuration Energy: 3.6742346142

Table 3. 5 Points

i	θ_i	ϕ_i	E_i
1	.0000	17.3540	2.621320
2	90.0000	.0000	2.568914
3	90.0000	120.0000	2.568914
4	90.0000	-120.0000	2.568914
5	180.0000	-49.4714	2.621320

Configuration Energy: 6.4746914947

Table 4. 6 Points

i	θ_i	ϕ_i	E_i
1	.0000	180.0000	3.328427
2	90.0000	.0000	3.328427
3	90.0000	90.0000	3.328427
4	90.0000	-180.0000	3.328427
5	90.0000	-90.0000	3.328427
6	180.0000	16.5044	3.328427

Configuration Energy: 9.9852813742

Table 5. 7 Points

i	θ_i	ϕ_i	E_i
1	.0000	.0000	4.035534
2	90.0000	.0000	4.166977
3	90.0000	72.0000	4.166977
4	90.0000	144.0000	4.166977
5	90.0000	-144.0000	4.166977
6	90.0000	-72.0000	4.166977
7	180.0000	45.0000	4.035534

Configuration Energy: 14.4529774142

Table 6. 8 Points

i	θ_i	ϕ_i	E_i
1	55.9140	45.0000	4.918822
2	55.9140	135.0000	4.918822
3	55.9140	-135.0000	4.918822
4	55.9140	-45.0000	4.918822
5	124.0860	.0000	4.918822
6	124.0860	90.0000	4.918822
7	124.0860	180.0000	4.918822
8	124.0860	-90.0000	4.918822

Configuration Energy: 19.6752878612

Table 7. 9 Points

i	θ_i	ϕ_i	E_i
1	45.2797	60.0001	5.707384
2	45.2794	-179.9999	5.707385
3	45.2795	-59.9999	5.707384
4	90.0000	.0000	5.758556
5	90.0000	120.0002	5.758556
6	90.0000	-120.0000	5.758555
7	134.7204	60.0001	5.707384
8	134.7206	-179.9999	5.707385
9	134.7204	-59.9999	5.707384

Configuration Energy: 25.7599865313

Table 8. 10 Points

i	θ_i	ϕ_i	E_i
1	.0000	-45.0000	6.593861
2	64.9956	.0000	6.530772
3	64.9956	90.0000	6.530772
4	64.9956	-180.0000	6.530772
5	64.9956	-90.0000	6.530772
6	115.0043	45.0000	6.530772
7	115.0044	135.0000	6.530772
8	115.0044	-135.0000	6.530772
9	115.0044	-45.0000	6.530772
10	180.0000	62.9003	6.593861

Configuration Energy: 32.7169494601

Table 9. 11 Points

i	θ_i	ϕ_i	E_i
1	.0000	.0000	7.320170
2	58.9820	.0000	7.460947
3	58.9820	-180.0000	7.460947
4	80.3075	60.2641	7.382462
5	80.3075	119.7359	7.382462
6	80.3075	-119.7359	7.382462
7	80.3075	-60.2641	7.382462
8	123.5512	.0000	7.365213
9	123.5512	-180.0000	7.365213
10	143.7026	90.0000	7.345281
11	143.7026	-90.0000	7.345281

Configuration Energy: 40.5964505082

Table 10. 12 Points

i	θ_i	ϕ_i	E_i
1	.0000	.0000	8.194209
2	63.4349	.0000	8.194209
3	63.4349	72.0000	8.194209
4	63.4350	144.0000	8.194209
5	63.4349	-144.0000	8.194209
6	63.4350	-72.0000	8.194209
7	116.5650	36.0000	8.194209
8	116.5651	108.0000	8.194209
9	116.5651	180.0000	8.194209
10	116.5651	-108.0000	8.194209
11	116.5651	-36.0000	8.194209
12	180.0000	-19.0575	8.194209

Configuration Energy: 49.1652530576

Table 11. 13 Points

i	θ_i	ϕ_i	E_i
1	30.3475	.0000	9.035459
2	30.3475	180.0000	9.035459
3	57.0005	90.0000	9.064802
4	57.0005	-90.0000	9.064802
5	84.0102	35.6849	9.056061
6	84.0103	144.3151	9.056061
7	84.0103	-144.3151	9.056060
8	84.0103	-35.6849	9.056060
9	120.0400	90.0000	8.955353
10	120.0400	-90.0000	8.955353
11	127.6831	.0000	9.117980
12	127.6831	180.0000	9.117980
13	180.0000	-114.6485	9.135031

Configuration Energy: 58.8532306117

Table 12. 14 Points

i	θ_i	ϕ_i	E_i
1	.0000	.0000	9.765716
2	62.9113	.0000	9.923442
3	62.9118	59.9997	9.923444
4	62.9115	119.9993	9.923442
5	62.9113	179.9993	9.923440
6	62.9114	-120.0006	9.923440
7	62.9110	-60.0004	9.923439
8	117.0890	29.9990	9.923444
9	117.0890	89.9993	9.923446
10	117.0886	149.9993	9.923443
11	117.0886	-150.0007	9.923439
12	117.0884	-90.0007	9.923436
13	117.0882	-30.0009	9.923440
14	180.0000	-92.1875	9.765716

Configuration Energy: 69.3063632968

Table 13. 15 Points

i	θ_i	ϕ_i	E_i
1	34.1857	-6.9635	10.768160
2	34.1857	113.0365	10.768160
3	34.1857	-126.9635	10.768160
4	65.9993	54.3779	10.788372
5	65.9993	174.3779	10.788372
6	65.9993	-65.6221	10.788372
7	90.0000	.0000	10.667099
8	90.0000	120.0000	10.667099
9	90.0000	-120.0000	10.667099
10	114.0007	65.6221	10.788372
11	114.0007	-174.3779	10.788372
12	114.0007	-54.3779	10.788372
13	145.8143	6.9635	10.768160
14	145.8143	126.9635	10.768160
15	145.8143	-113.0365	10.768160

Configuration Energy: 80.6702441143

Table 14. 16 Points

i	θ_i	ϕ_i	E_i
1	38.3161	45.0000	11.587574
2	38.3161	135.0000	11.587574
3	38.3161	-135.0000	11.587575
4	38.3160	-45.0000	11.587575
5	78.6587	-.0001	11.642515
6	78.6587	90.0000	11.642514
7	78.6587	-180.0000	11.642514
8	78.6587	-90.0000	11.642514
9	101.3413	44.9999	11.642514
10	101.3413	135.0000	11.642514
11	101.3413	-135.0000	11.642514
12	101.3414	-45.0000	11.642514
13	141.6840	.0001	11.587574
14	141.6839	90.0000	11.587574
15	141.6839	179.9999	11.587574
16	141.6840	-90.0000	11.587574

Configuration Energy: 92.9203539623

Table 15. 17 Points

i	θ_i	ϕ_i	E_i
1	.0000	-51.3402	12.480485
2	52.4425	36.0000	12.473493
3	52.4425	108.0000	12.473493
4	52.4425	180.0000	12.473493
5	52.4425	-108.0000	12.473493
6	52.4425	-36.0000	12.473493
7	90.0000	.0000	12.480982
8	90.0000	72.0000	12.480982
9	90.0000	144.0000	12.480982
10	90.0000	-144.0000	12.480982
11	90.0000	-72.0000	12.480982
12	127.5575	36.0000	12.473493
13	127.5575	108.0000	12.473493
14	127.5575	180.0000	12.473493
15	127.5575	-108.0000	12.473493
16	127.5575	-36.0000	12.473493
17	180.0000	-74.4601	12.480485

Configuration Energy: 106.0504048286

Table 16. 18 Points

i	θ_i	ϕ_i	e_i
1	.0000	−26.5650	13.395218
2	47.5344	44.9999	13.323511
3	47.5344	135.0002	13.323511
4	47.5344	−134.9996	13.323511
5	47.5345	−45.0000	13.323511
6	78.2636	.0000	13.348803
7	78.2633	90.0001	13.348799
8	78.2634	−179.9997	13.348800
9	78.2637	−89.9998	13.348804
10	101.7364	45.0001	13.348800
11	101.7363	135.0002	13.348797
12	101.7365	−134.9998	13.348803
13	101.7366	−44.9999	13.348805
14	132.4657	.0002	13.323514
15	132.4653	90.0002	13.323503
16	132.4655	−179.9999	13.323508
17	132.4659	−89.9999	13.323518
18	180.0000	111.9852	13.395218

Configuration Energy: 120.0844674476

Table 17. 19 Points

i	θ_i	ϕ_i	e_i
1	.0000	123.6901	14.135539
2	50.3259	60.0741	14.243828
3	50.3259	119.9259	14.243828
4	50.3259	−119.9259	14.243828
5	50.3259	−60.0741	14.243828
6	57.2964	.0000	14.155080
7	57.2964	180.0000	14.155079
8	94.0565	43.9990	14.284797
9	94.0565	136.0010	14.284797
10	94.0565	−136.0010	14.284797
11	94.0565	−43.9990	14.284797
12	101.3439	90.0000	14.164344
13	101.3439	−90.0000	14.164344
14	109.4347	.0000	14.284884
15	109.4347	−180.0000	14.284884
16	145.3941	−47.7365	14.180070
17	145.3941	47.7365	14.180070
18	145.3941	132.2635	14.180070
19	145.3941	−132.2635	14.180070

Configuration Energy: 135.0894675567

Table 18. 20 Points

i	θ_i	ϕ_i	e_i
1	.0000	170.5377	15.047828
2	46.0933	.0000	15.110163
3	46.0933	120.0000	15.110163
4	46.0933	−120.0000	15.110163
5	57.1649	60.0000	15.080704
6	57.1649	180.0000	15.080704
7	57.1649	−60.0000	15.080704
8	90.0000	25.0084	15.087047
9	90.0000	94.9916	15.087047
10	90.0000	145.0084	15.087047
11	90.0000	−145.0084	15.087047
12	90.0000	−94.9916	15.087047
13	90.0000	−25.0084	15.087047
14	133.9067	.0000	15.110163
15	133.9067	120.0000	15.110163
16	133.9067	−120.0000	15.110163
17	122.8350	60.0000	15.080704
18	122.8350	180.0000	15.080703
19	122.8350	−60.0000	15.080704
20	180.0000	−36.8699	15.047828

Configuration Energy: 150.8815683338

Table 19. 21 Points

i	θ_i	ϕ_i	e_i
1	.0000	.0000	16.001145
2	44.3205	90.0000	15.968753
3	44.3205	−90.0000	15.968753
4	44.5290	.0000	15.962009
5	44.5290	180.0000	15.962009
6	69.5805	45.1285	15.989869
7	69.5805	134.8715	15.989869
8	69.5805	−134.8715	15.989869
9	69.5805	−45.1285	15.989869
10	93.9647	90.0000	15.891518
11	93.9647	−90.0000	15.891518
12	94.1805	.0000	15.898412
13	94.1805	−180.0000	15.898412
14	113.9953	44.2417	16.002715
15	113.9953	135.7583	16.002715
16	113.9953	−135.7583	16.002715
17	113.9953	−44.2417	16.002715
18	145.3624	90.0000	15.980096
19	145.3624	−90.0000	15.980096
20	148.0701	.0000	15.955095
21	148.0701	180.0000	15.955095

Configuration Energy: 167.6416223993

Table 20. 22 Points

i	θ_i	ϕ_i	E_i
1	.0000	.0000	16.823093
2	43.3020	.0000	16.866652
3	43.3020	120.0000	16.866652
4	43.3020	-120.0000	16.866652
5	54.7356	60.0000	16.813813
6	54.7356	180.0000	16.813813
7	54.7356	-60.0000	16.813814
8	85.3696	23.4230	16.866652
9	85.3696	96.5770	16.866652
10	85.3696	143.4230	16.866652
11	85.3696	-143.4230	16.866652
12	85.3696	-96.5770	16.866652
13	85.3696	-23.4230	16.866652
14	109.4712	60.0000	16.823093
15	109.4712	180.0000	16.823093
16	109.4712	-60.0000	16.823093
17	125.2644	.0000	16.813813
18	125.2644	120.0000	16.813813
19	125.2644	-120.0000	16.813813
20	152.7732	60.0000	16.866651
21	152.7732	-180.0000	16.866651
22	152.7732	-60.0000	16.866652

Configuration Energy: 185.2875361493

Table 21. 23 Points

i	θ_i	ϕ_i	E_i
1	.0000	.0000	17.681113
2	43.0270	-10.6594	17.734784
3	43.0270	109.3406	17.734784
4	43.0270	-130.6594	17.734784
5	52.1498	52.3211	17.673754
6	52.1498	172.3211	17.673753
7	52.1498	-67.6789	17.673754
8	81.9146	10.8262	17.821185
9	81.9146	130.8262	17.821184
10	81.9146	-109.1738	17.821185
11	90.0000	90.0000	17.706609
12	90.0000	-150.0000	17.706609
13	90.0000	-30.0001	17.706609
14	98.0854	49.1737	17.821185
15	98.0854	169.1737	17.821184
16	98.0854	-70.8263	17.821185
17	127.8502	7.6788	17.673753
18	127.8502	127.6788	17.673753
19	127.8502	-112.3212	17.673753
20	136.9730	70.6593	17.734783
21	136.9730	-169.3407	17.734783
22	136.9730	-49.3407	17.734784
23	180.0000	-41.1161	17.681112

Configuration Energy: 203.9301906629

Table 22. 24 Points

i	θ_i	ϕ_i	E_i
1	30.5015	-29.5437	18.612257
2	30.5015	60.4563	18.612257
3	30.5015	150.4563	18.612256
4	30.5015	-119.5437	18.612257
5	75.5064	-27.1346	18.612257
6	116.2040	-16.1969	18.612256
7	63.7960	16.1969	18.612257
8	104.4936	27.1346	18.612256
9	75.5064	62.8654	18.612257
10	116.2040	73.8031	18.612256
11	104.4936	117.1346	18.612256
12	63.7960	106.1969	18.612256
13	75.5064	152.8654	18.612256
14	63.7960	-163.8031	18.612256
15	104.4936	-152.8654	18.612256
16	116.2040	163.8031	18.612255
17	63.7960	-73.8031	18.612257
18	75.5064	-117.1346	18.612256
19	116.2040	-106.1969	18.612256
20	104.4936	-62.8654	18.612256
21	149.4985	119.5437	18.612255
22	149.4985	29.5437	18.612256
23	149.4985	-60.4563	18.612256
24	149.4985	-150.4563	18.612256

Configuration Energy: 223.3470740518

Table 23. 25 Points

i	θ_i	ϕ_i	E_i
1	29.8458	44.4036	19.533207
2	29.8458	-44.4036	19.533207
3	30.3846	134.6633	19.476308
4	30.3846	-134.6633	19.476308
5	61.0208	.0000	19.545998
6	60.2249	-180.0000	19.453856
7	61.2361	84.1362	19.548009
8	61.2361	-84.1362	19.548009
9	73.7380	127.2608	19.457028
10	73.7380	-127.2608	19.457028
11	78.0093	41.6649	19.456136
12	78.0093	-41.6649	19.456136
13	99.1734	159.7334	19.587711
14	99.1734	-159.7334	19.587711
15	101.9396	85.3761	19.500784
16	101.9396	-85.3761	19.500784
17	102.0458	.0000	19.456121
18	119.4418	46.0856	19.508328
19	119.4418	-46.0856	19.508327
20	120.7382	123.1537	19.541763
21	120.7382	-123.1537	19.541763
22	142.0675	-180.0000	19.426132
23	144.6614	.0000	19.594481
24	156.0448	89.9375	19.465193
25	156.0448	-89.9375	19.465193

Configuration Energy: 243.8127602988

Table 24. 26 Points

i	θ_i	ϕ_i	E_i
1	25.4859	47.9039	20.348182
2	25.4859	-132.0961	20.348182
3	34.4236	145.6119	20.433831
4	34.4236	-34.3881	20.433832
5	55.4502	94.3909	20.508456
6	55.4502	-85.6091	20.508456
7	62.8512	6.4845	20.316368
8	62.8512	-173.5155	20.316368
9	71.9770	53.0021	20.350764
10	71.9770	-126.9979	20.350764
11	76.5747	135.1072	20.370649
12	76.5747	-44.8928	20.370649
13	95.4424	93.3488	20.407459
14	95.4424	-86.6512	20.407459
15	101.3843	165.7751	20.434347
16	101.3843	-14.2249	20.434347
17	102.0786	26.9536	20.453164
18	102.0786	-153.0464	20.453164
19	122.0164	-53.6803	20.354700
20	122.0164	126.3197	20.354700
21	122.9490	63.8795	20.393153
22	122.9490	-116.1205	20.393153
23	141.6506	4.4952	20.351644
24	141.6506	-175.5048	20.351644
25	159.0269	95.8726	20.410608
26	159.0269	-84.1274	20.410608

Configuration Energy: 265.1333263174

Table 25. 27 Points

i	θ_i	ϕ_i	E_i
1	.0000	.0000	21.280055
2	41.0744	.0000	21.254382
3	41.0745	72.0000	21.254382
4	41.0745	144.0000	21.254382
5	41.0745	-144.0000	21.254382
6	41.0744	-72.0000	21.254383
7	68.9658	36.0000	21.320088
8	68.9659	108.0000	21.320087
9	68.9659	180.0000	21.320087
10	68.9658	-107.9999	21.320088
11	68.9658	-36.0000	21.320087
12	90.0000	.0000	21.260085
13	90.0000	72.0000	21.260085
14	90.0001	144.0000	21.260085
15	89.9999	-144.0000	21.260085
16	90.0000	-72.0000	21.260085
17	111.0341	36.0000	21.320088
18	111.0342	108.0000	21.320088
19	111.0342	-179.9999	21.320087
20	111.0341	-108.0000	21.320087
21	111.0342	-35.9999	21.320087
22	138.9255	.0000	21.254382
23	138.9256	72.0000	21.254383
24	138.9256	144.0000	21.254382
25	138.9256	-144.0000	21.254382
26	138.9255	-72.0000	21.254381
27	180.0000	-49.2054	21.280054

Configuration Energy: 287.3026150330

Table 26. 28 Points

i	θ_i	ϕ_i	E_i
1	.0000	.0000	22.198715
2	37.8238	46.2811	22.223301
3	37.8237	-73.7189	22.223301
4	37.8237	166.2811	22.223301
5	48.0181	108.1219	22.125719
6	48.0181	-131.8781	22.125719
7	48.0181	-11.8781	22.125718
8	109.4712	60.0000	22.198715
9	72.6404	68.7646	22.223301
10	115.1753	19.4263	22.223300
11	131.5199	96.2956	22.223300
12	75.8252	25.1899	22.125719
13	155.3402	38.4866	22.125718
14	90.2851	104.9503	22.125719
15	109.4712	-180.0000	22.198714
16	115.1753	139.4263	22.223300
17	72.6404	-171.2354	22.223300
18	131.5200	-143.7044	22.223300
19	155.3402	158.4865	22.125718
20	90.2851	-135.0497	22.125719
21	75.8252	145.1899	22.125718
22	109.4712	-60.0000	22.198715
23	115.1753	-100.5737	22.223301
24	72.6404	-51.2354	22.223301
25	131.5199	-23.7044	22.223300
26	155.3402	-81.5134	22.125718
27	75.8252	-94.8101	22.125719
28	90.2851	-15.0497	22.125718

Configuration Energy: 310.4915423582

Table 27. 29 Points

i	θ_i	ϕ_i	E_i
1	.0000	.0000	23.144347
2	36.3913	61.9049	23.144303
3	36.3913	-178.0951	23.144303
4	36.3913	-58.0951	23.144303
5	48.1058	2.6916	23.018771
6	48.1058	122.6916	23.018771
7	48.1058	-117.3084	23.018771
8	71.2866	83.5921	23.112166
9	71.2866	-156.4079	23.112166
10	71.2866	-36.4079	23.112166
11	72.4492	40.5265	23.065308
12	72.4492	160.5265	23.065308
13	72.4492	-79.4735	23.065308
14	90.0000	.0000	22.978967
15	90.0000	120.0000	22.978967
16	90.0000	-120.0000	22.978967
17	107.5508	79.4735	23.065308
18	107.5508	-160.5265	23.065308
19	107.5508	-40.5265	23.065308
20	108.7134	36.4079	23.112166
21	108.7134	156.4079	23.112166
22	108.7134	-83.5921	23.112166
23	131.8942	117.3084	23.018771
24	131.8942	-122.6916	23.018771
25	131.8942	-2.6916	23.018771
26	143.6087	58.0951	23.144302
27	143.6087	178.0951	23.144302
28	143.6087	-61.9049	23.144302
29	180.0000	-28.8968	23.144347

Configuration Energy: 334.6344399204

Table 28. 30 Points

i	θ_i	ϕ_i	E_i
1	.0000	-16.5260	23.963386
2	39.0170	61.4676	24.031289
3	39.0170	-118.5324	24.031289
4	39.8800	177.5102	24.028857
5	39.8800	-2.4898	24.028857
6	43.9651	121.1991	23.966266
7	43.9651	-58.8009	23.966266
8	69.3551	31.1097	23.956473
9	69.3551	-148.8903	23.956474
10	72.0211	82.7757	23.956351
11	72.0211	-97.2243	23.956352
12	75.7442	165.8784	23.923154
13	75.7442	-14.1216	23.923155
14	80.8672	124.9512	23.957887
15	80.8672	-55.0488	23.957888
16	99.1332	55.0479	23.957886
17	99.1332	-124.9521	23.957886
18	104.2554	14.1208	23.923155
19	104.2554	-165.8792	23.923155
20	107.9791	-82.7765	23.956356
21	107.9791	97.2235	23.956356
22	110.6447	148.8900	23.956476
23	110.6447	-31.1100	23.956477
24	136.0352	58.8007	23.966271
25	136.0352	-121.1993	23.966271
26	140.1197	2.4898	24.028852
27	140.1197	-177.5102	24.028852
28	140.9829	118.5326	24.031287
29	140.9830	-61.4673	24.031287
30	180.0000	34.6411	23.963380

Configuration Energy: 359.6039459038

Table 29. 31 Points

i	θ_i	ϕ_i	E_i
1	.0000	90.0000	24.823572
2	38.0847	.0000	24.892075
3	38.0847	120.0000	24.892075
4	38.0847	-120.0000	24.892075
5	42.6863	60.0000	24.843089
6	42.6863	-60.0000	24.843089
7	42.6863	-180.0000	24.843088
8	71.4639	23.4627	24.860789
9	71.4639	96.5373	24.860789
10	71.4639	143.4627	24.860788
11	71.4639	-143.4627	24.860788
12	71.4639	-96.5373	24.860789
13	71.4639	-23.4627	24.860789
14	82.0676	60.0000	24.904643
15	82.0676	-180.0000	24.904643
16	82.0676	-60.0000	24.904643
17	99.6599	.0000	24.931904
18	99.6599	120.0000	24.931904
19	99.6599	-120.0000	24.931904
20	114.3095	39.0010	24.827434
21	114.3095	80.9990	24.827434
22	114.3095	159.0010	24.827433
23	114.3095	-159.0010	24.827433
24	114.3095	-80.9990	24.827434
25	114.3095	-39.0010	24.827434
26	136.7842	.0000	24.983097
27	136.7842	120.0000	24.983097
28	136.7842	-120.0000	24.983097
29	155.2769	60.0000	24.814782
30	155.2769	180.0000	24.814782
31	155.2769	-60.0000	24.814782

Configuration Energy: 385.5308380633

Table 30. 32 Points

i	θ_i	ϕ_i	E_i
1	37.3774	36.0000	25.744732
2	37.3774	107.9999	25.744732
3	37.3773	180.0000	25.744732
4	37.3774	-108.0000	25.744733
5	37.3774	-36.0000	25.744733
6	79.1877	36.0000	25.744733
7	79.1877	108.0000	25.744732
8	79.1877	180.0000	25.744732
9	79.1876	-108.0000	25.744733
10	79.1877	-36.0000	25.744733
11	100.8123	.0001	25.744733
12	100.8124	72.0000	25.744733
13	100.8123	144.0000	25.744732
14	100.8123	-144.0000	25.744731
15	100.8123	-71.9999	25.744733
16	142.6227	.0001	25.744735
17	142.6227	72.0001	25.744734
18	142.6226	144.0001	25.744730
19	142.6225	-143.9999	25.744727
20	142.6226	-72.0000	25.744730
21	.0000	.0000	25.802325
22	63.4349	.0000	25.802326
23	63.4350	72.0000	25.802326
24	63.4349	144.0000	25.802325
25	63.4349	-144.0000	25.802325
26	63.4349	-72.0000	25.802327
27	116.5651	36.0001	25.802327
28	116.5651	108.0001	25.802326
29	116.5650	-179.9999	25.802325
30	116.5650	-107.9999	25.802324
31	116.5651	-35.9999	25.802326
32	180.0000	-147.3426	25.802324

Configuration Energy: 412.2612746506

Table 31. 36 Points

i	θ_i	ϕ_i	E_i
1	17.6304	153.9305	29.361568
2	17.6304	-26.0695	29.361569
3	162.3696	-153.9311	29.361565
4	162.3696	26.0689	29.361565
5	34.2935	-130.4051	29.381117
6	34.2935	49.5949	29.381117
7	145.7064	130.4050	29.381114
8	145.7064	-49.5950	29.381114
9	44.2720	101.8136	29.449404
10	44.2720	-78.1864	29.449404
11	135.7282	-101.8137	29.449405
12	135.7282	78.1863	29.449405
13	53.3378	148.5307	29.458690
14	53.3378	-31.4693	29.458691
15	126.6622	-148.5307	29.458692
16	126.6622	31.4693	29.458693
17	57.3654	-171.0748	29.382784
18	57.3654	8.9252	29.382785
19	122.6345	171.0749	29.382784
20	122.6345	-8.9251	29.382786
21	69.3586	-133.9493	29.421524
22	69.3586	46.0507	29.421524
23	110.6412	133.9496	29.421528
24	110.6412	-46.0504	29.421528
25	73.8685	-97.4411	29.409713
26	73.8685	82.5589	29.409713
27	106.1318	97.4413	29.409711
28	106.1318	-82.5587	29.409711
29	78.0238	121.5818	29.389079
30	78.0238	-58.4182	29.389080
31	101.9762	-121.5817	29.389078
32	101.9762	58.4182	29.389078
33	86.8113	162.0963	29.307324
34	86.8113	-17.9037	29.307325
35	93.1886	-162.0961	29.307323
36	93.1886	17.9039	29.307324

Configuration Energy: 529.1224083754

Table 32. 8 Points (Cube)

i	θ_i	ϕ_i	E_i
1	54.7356	45.0000	4.935194
2	54.7356	135.0000	4.935193
3	54.7356	-135.0000	4.935193
4	54.7356	-45.0000	4.935194
5	125.2644	45.0000	4.935193
6	125.2644	135.0000	4.935193
7	125.2644	-135.0000	4.935193
8	125.2644	-45.0000	4.935193

Configuration Energy: 19.7407740738

Table 33. 20 Points (Regular Dodecahedron)

i	θ_i	ϕ_i	E_i
1	37.3774	36.0000	15.179862
2	37.3774	108.0000	15.179862
3	37.3774	180.0000	15.179862
4	37.3774	-108.0000	15.179861
5	37.3774	-36.0000	15.179862
6	79.1877	36.0000	15.179862
7	79.1877	108.0000	15.179863
8	79.1877	180.0000	15.179862
9	79.1877	-108.0000	15.179861
10	79.1877	-36.0000	15.179862
11	100.8123	.0000	15.179862
12	100.8123	72.0000	15.179863
13	100.8123	144.0000	15.179863
14	100.8123	-144.0000	15.179862
15	100.8123	-72.0000	15.179862
16	142.6226	.0000	15.179862
17	142.6226	72.0000	15.179862
18	142.6226	144.0000	15.179863
19	142.6226	-144.0000	15.179862
20	142.6226	-72.0000	15.179862

Configuration Energy: 151.7986205619

Table 34. 32 Point Anomalous Configuration

i	θ_i	ϕ_i	E_i
1	25.6881	.0000	25.810951
2	25.6881	90.0000	25.810952
3	25.6881	180.0000	25.810951
4	25.6881	-90.0000	25.810951
5	57.0005	45.0000	25.706294
6	57.0005	135.0000	25.706294
7	57.0005	-135.0000	25.706294
8	57.0005	-45.0000	25.706294
9	61.2989	.0000	25.864476
10	61.2989	90.0000	25.864477
11	61.2989	180.0000	25.864476
12	61.2989	-90.0000	25.864476
13	90.0000	22.5000	25.735377
14	90.0000	67.5000	25.735378
15	90.0000	112.5000	25.735377
16	90.0000	157.5000	25.735377
17	90.0000	-157.5000	25.735377
18	90.0000	-112.5000	25.735377
19	90.0000	-67.5000	25.735377
20	90.0000	-22.5000	25.735377
21	118.7011	45.0000	25.864477
22	118.7011	135.0000	25.864476
23	118.7011	-135.0000	25.864477
24	118.7011	-45.0000	25.864476
25	122.9995	90.0000	25.706294
26	122.9995	-180.0000	25.706295
27	122.9995	-90.0000	25.706294
28	122.9995	.0000	25.706294
29	154.3119	45.0000	25.810951
30	154.3119	135.0000	25.810952
31	154.3119	-135.0000	25.810952
32	154.3119	-45.0000	25.810952

Configuration Energy: 412.4683971952

LITERATURE CITED

1. Melnyk, T.W., Knop, O., and Smith, W.R. *Extremal Arrangements of Points and Unit Charges on a Sphere.* Can. J. Chem. *53*, 1745-1761 (1977).

2. Clare, B.W., and Kepert, D.L. *The Closest Packing of Equal Circles on a Sphere.* Proc. Roy. Soc. Lond. *A405*, 329-344 (1986).

3. Segre, B., and Mahler, K. *On the Densest Packing of Circles.* Amer. Math. Monthly *51*, 261-270 (1944).

4. Berezin, A.A. *Asymptotics of the Maximum Number of Repulsive Particles on a Spherical Surface.* J. Math. Phys. *27(6)*, 1533-1536 (1912).

5. Foeppl, L. J. Reine Angew. Math. *141*, 2511 (1912).

6. Berezin, A.A. *Simple Electrostatic Model of the Structural Phase Transition.* Am. J. Phys. *54(5)*, 403-4055 (1986).

END

6-87

DTIC